Study on molecular evolution and population genetic features on Blakiston's fish owl

（シマフクロウにおける分子進化および集団遺伝学的特徴に関する研究）

Department of Natural History Sciences,

Graduate School of Science, Hokkaido University

北海道大学 大学院 理学院 自然史科学専攻

OMOTE Keita

表　渓太

2016 年 3 月

Contents

Abstract

Blakiston's fish owl (*Bubo blakistoni*), the largest owl endemic to northeastern Asia, comprises two subspecies: *B. b. doerriesi* in continental Eurasia and *B. b. blakistoni* on Hokkaido Island and the southern Kuril islands. Although Blakiston's fish owl was formerly widespread on Hokkaido Island, its population size decreased during the 20th century due to reduction and fragmentation of its habitat through human activities.

The phylogenetic analyses based on the whole mitochondrial DNA (mtDNA) sequences revealed a deep separation between continental and insular subspecies, which diverged an estimated 670 kilo years before present. The divergence times among haplotypes within each subspecies showed that severer bottlenecks and subsequent founder events occurred at least during the last glacial period. The whole mtDNA genome, which included duplicated genes, was the largest (>21 kilo base-pairs, kbp) in vertebrates to data. The large tandem repeat sequences were found in the control region of *B. blakistoni* and the closest related species of *Bubo*.

To elucidate the temporal and spatial changes in population structure and genetic diversity, 439 individuals including old museum samples were collected for the last 100 years. I detected a population bottleneck and fragmentation event by mtDNA haplotype and microsatellite analyses. The effective population size, which was estimated by moment and temporal methods from microsatellite data, showed the lowest value in 1980s. Most haplotypes were previously widespread across Hokkaido, but have become fixed in separate areas after the bottleneck period. Genetic

differentiations among local populations was indicated from both mtDNA and microsatellite data, and likely arose through population fragmentation.

In addition, the copy numbers of the major histocompatibility complex (MHC) genes, whose variations relate to resistance against pathogens, were analyzed to reveal the evolutionary pattern. The results of quantitative real-time PCR and massively parallel pyrosequencing showed suggested a higher level of MHC loci in *B. blakistoni* than other owl species. The results of fluorescence in situ hybridization showed that the locations of MHC class I and class IIß loci were closely linked on a micro-chromosomes, indicating that the MHC loci were tandemly duplicated in a limited chromosome regions. The gene duplication increases the variations of MHC genes in this owl species, and could have improved adaptation of the tiny populations to the island and cold climates.

General Introduction

Blakiston's fish owl (*Bubo blakistoni*), the largest owl endemic to northeastern Asia, comprises two subspecies: *B. b. doerriesi* in continental Eurasia and *B. b. blakistoni* on Hokkaido Island and the southern Kuril Islands (Slaght & Surmach 2008). This species is resident in riparian forests and needs a large quantity of fish for food and large hollow trees for nesting (Takenaka 1998; Yamamoto 1999). It can reach age of over 20 years and inhabits restricted territories along rivers; the clutch size is usually two (Hayashi 1997; Yamamoto 1999). Although Blakiston's fish owl was formerly widespread in forests on Hokkaido Island, its population size decreased during the 20th century due to reduction and fragmentation of its habitat through human activities. There have been no records of this owl in southern Hokkaido since the 1950s, in northern Hokkaido since the 1970s, or in the Ishikari lowlands since the 1980s (Hayashi 1999). Today Blakiston's fish owl survives only in eastern Hokkaido, where the population has declined since the 1970s, and the total population size on Hokkaido in the 1980s was estimated to be less than 100 individuals by field researches (Brazil & Yamamoto 1989; Takenaka 1998). For this reason, Blakiston's fish owl has been listed as endangered on the IUCN Red List Ver.3.1, and as a National Endangered Species under Japanese law. Recent field researches showed that, due to conservation efforts involving artificial nesting and feeding, the population has recovered to about 140 individuals in limited areas on Hokkaido. During the last 25 years, most young owls from known nest locations have been leg-banded through conservation activities by the

Japanese government. Familial relationships and dispersal patterns are known for several individuals; movements of a few individuals among areas have been observed since the 1990s (T. Takenaka, unpublished data).

Genetic information such as genetic diversity, history of population structure, and relationships among the subspecies is needed to carry conservation activities for the endangered species. In the present study, the purposes are to reveal phylogeny of Blakiston's fish owl in genus *Bubo* (Chapter I), discuss phylogeography on northeast Asia (Chapter II), reveal temporal changes of genetic diversity and structure in the Hokkaido population (Chapter III), and investigate variation and molecular evolution of the major histocompatibility complex (Chapter IV).

Chapter I

Phylogenetic relationships in *Bubo* species based on the mitochondrial DNA control region sequences

Introduction

Genus *Bubo* in Family Strigidae comprises large owl species distributed in many parts of the world. Wink et al. (2009) reconstructed an owl phylogeny based on mitochondrial cytochrome *b* (cyt *b*) and nuclear *RAG-1* sequences and found *Nyctea*, *Scotooelia*, and *Ketupa* to be embedded within a *Bubo* clade, which supported previous conclusions that these three genera should be included in *Bubo* (e.g., König & Weick 2008). The former genus *Ketupa* included four species: Blakiston's fish owl (*B. blakistoni*), buffy fish owl (*B. ketupu*), tawny fish owl (*B. flavipes*), and brown fish owl (*B. zeylonesis*). Wink et al. (2009) did not include *B. blakistoni* and *B. flavipes* in their phylogenetic analysis.

The mtDNA control region is the major non-coding element and one of the most variable regions in vertebrate mtDNA (Wenink et al. 1994). The size of the mtDNA control region varies considerably in vertebrates, resulting mainly from variation in the occurrence and number of tandem repeats. In birds, the mtDNA control region is usually 1–1.5 kilo base-pairs (kbp) long, located between the $tRNA^{Glu}$ and $tRNA^{Phe}$ genes, and comprises three domains that include several conserved regions (Roukonen & Kvist 2002). Although much of the variation consists of nucleotide substitutions and insertions and deletions (indels), considerable length variation among species can occur due to tandemly repeated units in the third domain, with units ranging in size from four to hundreds of base pairs, and in number from two to more than 100 copies (Lunt et al. 1998). As in other vertebrate groups, species with a tandem repeat region also have a longer control region

overall, with the longest previously reported in birds being 3290 bp in the short-eared owl (*Asio flammeus*) (Xiao et al. 2006). In this chapter, the phylogeny of *B. blakistoni* and other fish owl species in *Bubo* is discussed based on mtDNA sequences and the patterns of tandem repeat in control region.

Materials and methods

Samples and DNA extraction

Total DNA was extracted from blood or cultured fibroblasts from 20 *B. blakistoni* individuals captured on Hokkaido Island, Japan, and from cultured fibroblasts or feather roots from another eight *Bubo* species and an outgroup taxon: *B. ketupu* and *B. flavipes* (formerly included in *Ketupa*), Verreaux's eagle-owl (*B. lacteus*), spot-bellied eagle-owl (*B. nipalensis*), barred eagle-owl (*B. sumatranus*), Eurasian eagle-owl (*Bubo bubo*), great horned owl (*B. virginianus*), snowy owl (*B. scandiacus*), and Ural owl (*Strix uralensis*; outgroup) (Table 1-1). Blood samples were preserved in ethanol or dried on filter paper, and frozen at -20°C until use. Fibroblasts were cultured from skin tissue and frozen in liquid nitrogen until use. Total DNA was extracted from blood and fibroblasts by using the DNeasy Blood & Tissue Kit (Qiagen), and from feather roots by using the QIAamp DNA Micro Kit (Qiagen).

DNA amplification and sequencing

The polymerase chain reaction (PCR) primers for amplification of

the mtDNA control region and cyt *b* gene were designed de novo, or were modified from primers previously reported by Sorenson et al. (1999) (Table 1-2). The PCRs were performed by using PrimeSTAR GXL DNA Polymerase (Takara); cycling conditions were 35 cycles of 98°C for 10 sec, 60°C for 15 sec, and 68°C for 1 min; products were stored at 4°C. The PCR products were separated, and their molecular sizes were estimated, by electrophoresis on 2% agarose gels; they were purified with the QIAquick PCR Purification Kit (Qiagen) and used as templates for nucleotide sequencing. Sequencing was performed with an ABI 3130 or 3730 DNA automated sequencer. To detect artifacts, the repeat region from each individual was sequenced at least twice from independent PCR products. Sequences obtained have been deposited in the DDBJ/GenBank/EMBL databases under accession numbers AB741537–AB741546 and AB743785–AB743800.

Sequence data analyses

Sequences were aligned by using MEGA 5.0 software (Tamura et al. 2011). Gene locations were determined by comparisons with mtDNA control region and cyt *b* sequences from chicken (*Gallus gallus*; accession no. NC001323; Valverde et al. 1994), southern boobook (*Ninox novaeseelandiae*; NC005932; Harrison et al. 2004), and spotted owl (*Strix occidentalis*; AY833623; Barrowclough et al. 2005). An alignment of control region sequences was referred to the following sequence blocks conserved in avian mtDNA (Roukonen & Kvist 2002): extended termination-associated sequences 1 and 2 (ETAS-1 and ETAS-2); B-box, C-box, D-box, E-box, F-box;

and conserved sequence box 1 (CSB-1). The control region comprises three domains defined by variability and nucleotide composition (Saccone et al. 1991); the second domain was defined to begin with the F-box, and the third domain to begin with CSB-1.

Phylogenetic trees for the control region (1282 bp, excluding indels), complete cyt *b* (1140 bp), and combined control region + cyt *b* data sets, including nine ingroup taxa and *Strix uralensis* as the outgroup, were reconstructed by maximum likelihood implemented in TREEFINDER March 2011 (Jobb et al. 2004). A partition homogeneity test performed in PAUP 4.0 (Swofford 2002) indicated that the two genes did not contain significantly different phylogenetic signals ($P = 0.68$). Since analyses of the three data sets gave identical tree topologies, with the combined analysis having the highest nodal support values, only the combined analysis was described in the text. The optimal substitution model for the combined data set determined with MEGA 5.0 was HKY+GI. The robustness of nodes was assessed from analyses of 1000 bootstrap pseudoreplicates.

To examine more extensively relationships among species formerly placed in *Ketupa*, a maximum-likelihood analysis was conducted based on 1001 bp of cyt *b* that included an additional six *Bubo* species over the combined analysis above, for which sequences were obtained from GenBank: pharaoh eagle-owl (*B. ascalaphus*; EU348976), cape eagle-owl (*B. capensis*; EU348978), Indian eagle-owl (*B. bengalensis*; AJ003954), spotted eagle-owl (*B. africanus*; AJ003952), lesser horned owl (*B. magellanicus*; AJ003971), and brown fish owl (*B. zeylonesis*; EU348975) (Wink et al. 2009). The

optimal substitution model determined with MEGA 5.0 for the expanded cyt *b* data set was HKY+G.

Results

Phylogenetic relationships among *Bubo* species

The maximum likelihood tree for the control region (1282 bp) and complete cyt *b* sequences (1140 bp) combined (Fig. 1-1), and the maximum likelihood tree for partial cyt *b* sequences (1001 bp) but including additional species (Fig. 1-2), both show *Bubo* divided into two main clades (Clades 1 and 2, Fig. 1-2). Nodal support for these clades was generally high, 89–100% for Clade 1 and 99% for Clade 2. The tree in Fig. 1-2 (cyt *b*; more taxa) differs in topology for the comparable nodes in Fig. 1-1 (combined control region and cyt *b*; fewer taxa) in that the three main branches in Clade 1 form an unresolved trichotomy, and *B. ketupu is* the sister group to *B. blakistoni* rather than to *B. flavipes*. In both trees, species formerly placed in *Ketupa* form a well-supported (99–100%) '*Ketupa* clade', with the relationships among the species in this clade (Fig. 1-2) weakly supported, except for the sister group relationship between *B. flavipes* and *B. zeylonensis* in Fig. 1-2. Clade 1 consists of Asian species, with the exception of *B. lacteus* in Africa.

Organization of the *Bubo* mtDNA control region

The complete control region sequences (1478–1729 bp long) were from *B. bubo*, *B. virginianus*, *B. scandiacus*, *B. nipalensis*, *B. sumatranus*, and *S. uralensis*. By contrast, it was impossible to completely sequence the

central part of the third domain in *B. blakistoni*, *B. ketupu*, *B. flavipes*, and *B. lacteus*, due to an extended region of tandem repeats roughly 3.0–3.8 kbp long (Fig.1-3), estimated from gel electrophoresis.

The control region in all species examined contained conserved sequence blocks: ETAS-1 and ETAS-2 in the first domain; B-box, C-box, D-box, E-box and F-box in the second domain; and CSB-1 in the third domain (Fig.1-3). In the first domain, there were many indels and incomplete repeated sequences, most of which were 22 bp long and similar to part of ETAS-2. The first domain in *B. lacteus* contained a unique insertion of more than 100 bp. The second domain was more highly conserved in sequence than the other domains. The repeat region toward the 3' end of the third domain in *B. blakistoni*, *B. ketupu*, *B. flavipes*, and *B. lacteus* contained an estimated 20–25 copies of units 77 or 78 bp long; the nucleotide sequences of these units were 80.6–98.5% similar among the four species. By contrast, the third domain in *B. nipalensis*, *B. sumatranus*, *B. bubo*, *B. virginianus*, *B. scandiacus*, and *S. uralensis* contained no complete tandem repeats, but did contain at the same locus a sequence motif 72–82 bp long that was similar to the repeated sequences in the four *Bubo* species having tandem repeats. Similarity between tandem repeat units and non-repeated homologous loci in species lacking a cluster was 56.7–79.1%. The control region in *S. uralensis* contained three and four copies of incomplete repeat units in two individuals.

Discussion

Phylogenetic relationships in *Bubo*

The phylogenies in Figs. 1-1 and 1-2 based on mtDNA control region and cyt *b* sequences showed *Bubo* subdivided into two main clades (designated Clades 1 and 2), with species formerly in *Ketupa* included in Clade 1. The analyses, however, failed to adequately resolve sister-group relationships among members of the well-supported *Ketupa* clade (99% nodal support in the cyt *b* tree, Fig.1-2), with low support values at relevant nodes. This suggests that these three Asian species diverged rapidly or relatively recently, and additional markers will be necessary to resolve the relationships among them.

Among the *Bubo* species for which I examined the control region (Fig.1-3), a long stretch of tandem repeats was found only in four species in Clade 1; *B. nipalensis* and *B. sumatranus* in this clade lacked tandem repeats. The interpretation of this pattern is that duplications of an ancestral repeat unit and the expansion of a cluster occurred independently in each species. Arguing against this interpretation is the presence of a repeat cluster in three species (*B. blakistoni*, *B. flavipes*, and *B. ketupu*) comprising a clade within the well-supported *Ketupa* clade (Figs. 1-1 and 1-2), the most parsimonious explanation for which is that the common ancestor also had a repeat cluster. An explanation reconciling these apparently contradictory results is that an ancestral cluster was present, but that the repeat units within each species have undergone concerted evolution through gene conversion (Chen et al. 2007), rendering paralogs more similar to one another within a species than between species.

Chapter II

Phylogeography on the continental and island populations of Blakiston's fish owl, in northeastern Asia

Introduction

Blakiston's fish owl (*Bubo blakistoni*) is endemic to northeastern Asia. *B. blakistoni* constitutes a closely related monophyletic group with the tawny fish owl (*B. flavipes*), buffy fish owl (*B. ketupu*) and brown fish owl (*B. zeylonesis*) (Omote et al. 2013). Although these four fish owl species have morphological and ecological characteristics similar to each other, only *B. blakistoni* lives in boreal forests, and the others live in tropical or subtropical forests in southern Asia. The distribution of *B. blakistoni* has been fragmented in the Russian Far East, northeastern China and northern Japan (Fig. 2-1). There are two generally recognized subspecies: an island subspecies *B. b. blakistoni*, which occurs on Hokkaido Island and Kunashir and Shikotan Islands of the southern Kuril Islands; and a mainland species *B. b. doerriesi*, which ranges in the continent from southern Mgadan to Primorye and northeastern China (Slaght & Surmach 2008). Although Blakiston's fish owl was previously reported to be distributed on Sakhalin Island before 1969, a survey in 2005 did not confirm their current occurrence there (Slaght & Surmach 2008). There has been no genetic data for the species on the Eurasian Continent, Sakhalin and southern Kuril Islands. In this chapter, I determined nucleotide sequences of the complete mitochondrial genomes to analyze the phylogenetic relationships among subspecies from continental and insular areas, and discuss the phylogeographic patterns and historical demographic events in northeastern Aisa.

Materials and Methods

Whole mitochondrial DNA sequencing

For sequencing the whole mtDNA genome of *B. blakistoni*, I utilized blood, tissue, and feather samples from Russia (six samples) and 10 blood samples from Hokkaido. I used *B. flavipes*, a closely related species distributed in southeastern Asia, as an outgroup taxon: to obtain the DNA, fibroblasts were cultured from a skin sample obtained from the Ueno Zoological Gardens. Blood and tissue samples were preserved in ethanol at -20°C until use. Total DNA was extracted from blood, tissue or fibroblasts by using the DNeasy Blood & Tissue Kit (Qiagen), and from feather roots by using the QIAamp DNA Micro Kit (Qiagen).

The whole mitochondrial genomes were amplified from total DNA in six overlapping fragments (2.5–7.8 kbp) by PCR using PrimeSTAR GXL DNA Polymerase (Takara). The PCR cycling conditions were 98°C for 3 min; 30 cycles of 98°C for 10 sec, 60°C for 15 sec, and 68°C for 15 sec to 3 min; and 72°C for 10 min. The PCR products to be used as templates for nucleotide sequencing were purified with the QIAquick PCR Purification Kit (Qiagen). Sequencing was performed with the BigDye Terminator 3.1 Cycle Sequencing Kit and an ABI 3730 DNA automated sequencer (Applied Biosystems). Primers for PCR and sequencing (Table 2-1) were newly designed, or used or modified from those in Sorenson et al. (1999) and Omote et al. (2013). Nucleotide sequences were aligned by using MEGA 5.0 software (Tamura et al. 2011). The whole mtDNA sequences of *B. blakistoni* and *B. flavipes* were deposited in GenBank: accession nos. LC099100–LC099107.

Phylogenetic analysis

To examine the phylogenetic relationships among mtDNA haplotypes and divergence times between clades, I used the sequences of all 13 protein-coding genes (11,373 bp), because extensive sequence data were required for the accurate estimation of branch lengths among the closely related lineages. The 13 protein-coding sequences were obtained from three continental and four insular individuals, from samples from Primorye, Amur and Hokkaido Island. In addition, the entire sequence of the mitochondrial genome (including the 13 coding genes) was determined for *B. flavipes*, as an outgroup taxon. Because two duplicated genes (cytochrome *b*-2 and ND6-2) were each identical in sequences within individuals, one set was removed from subsequent molecular phylogenetic analyses.

Phylogenetic trees were reconstructed with the maximum likelihood method implemented with Treefinder March 2011 software (Jobb et al. 2004), and by Bayesian inference implemented with BEAST 1.6.2 software (Drummond et al. 2006; Drummond & Rambaut 2007). The best-fit model of substitution was determined independently for each of the 13 protein-coding genes by using MEGA 5.0. A Bayesian skyline model or a coalescent constant size model was used as a tree prior. A posterior set of trees was obtained through the Bayesian MCMC analysis, which was run for 10,000,000 interactions. The Bayesian analysis was used to estimate the divergence times between and within the continental and insular populations using a strict clock model. To calculate the divergence times among haplotypes, I

used 1.2% per million years as the evolutionary rate of all mitochondrial coding genes according to those in Accipitridae (Eo & DeWoody 2010).

Haplotyping of mitochondrial DNA sequences

For revealing geographic distributions of mtDNA haplotypes, I utilized blood, tissue, feather, and skull samples from Russia (34 samples from Primorye, two from the Amur region, and one from Magadan); and feathers obtained from stuffed specimens from Kunashir Island in the southern Kuril Islands (two samples) and Sakhalin Island (one sample), which were collected in 1928 before there disappearance in Sakhalin. On Hokkaido Island, the population structure could have been changed due to habitat fragmentation and reduction caused by human activities. To reconstruct the structure of the Hokkaido population before this disturbance, sequence data obtained in Omote et al. (2015) was used from museum specimens (19 samples) collected before 1980. Stuffed specimens had been housed in museums or research institutes in Japan. Total DNA was extracted from blood or tissue by using the DNeasy Blood & Tissue Kit (Qiagen), and from feather roots by using the QIAamp DNA Micro Kit (Qiagen). Total DNA was extracted from a partial skull sample by using the method of Masuda et al. (2001).

Sequencing from the DNA samples was performed on shorter fragments (140–590 bp), amplified by using the Multiplex PCR Master Mix (Qiagen): the PCR cycling conditions were 95°C for 15 min; 40 cycles of 94°C for 30 sec, 57°C for 3 min and 72°C for 30 sec; and 72°C for 10 min. The PCR

products to be used as templates for nucleotide sequencing were purified with the QIAquick PCR Purification Kit (Qiagen). Sequencing was performed with the BigDye Terminator 1.1 Cycle Sequencing Kit and an ABI 3730 DNA automated sequencer (Applied Biosystems). Haplotypes of the samples were assigned based on the nucleotide sequences of mitochondrial control region 2 (CR-2), using the criteria for haplotyping specified in Omote et al. (2015).

Nuclear microsatellite analysis

To estimate the genetic diversity for nuclear genes in continental individuals, 34 samples from Primorye (fresh blood or other tissues) were genotyped using seven autosomal microsatellite loci, according to the method of Omote et al. (2015). Alleles were defined by the molecular size of PCR products as determined with an ABI 3730 DNA automated sequencer using the GS600 LIZ size standard and GENEMAPPER 4.0 software (Applied Biosystems). Tests for departure from Hardy-Weinberg equilibrium and calculations of observed (*H*o) and expected (*H*e) heterozygosities were performed with ARLEQUIN 3.5.1.2 software (Excoffier & Lischer 2010).

Results

Organization of the whole mitochondrial genes of *Bubo blakistoni*

The size of the whole mitochondrial genome of *B. blakistoni* was at least 21 kbp. The genome contained a tandemly duplicated gene unit from the cytochrome *b* (cytb) to control region (CR); due to sequencing difficulties

and resulting ambiguity in the large tandemly duplicated repeat region in CR-2, it was unable to determine the exact size of the genome. In the duplicated repeat region, only cytb gene sequences were partial, and the sequences of $tRNA^{Thr}$-2, $tRNA^{Pro}$-2, $tRNA^{Glu}$-2 and ND6-2 were identical with those of $tRNA^{Thr}$-1, $tRNA^{Pro}$-1, $tRNA^{Glu}$-1 and ND6-1. Both CR-1 and CR-2 included tandem repeats consisting of four to six copies of 49-bp units (51-bp units in *B. flavipes*), whereas only CR-2 had a much longer tandem repeat region consisting of more than 20 times of 78-bp or 79-bp units. There were variations in the number and/or order of tandem repeat units as reported in Omote et al. (2013). Sequence regions other than the tandem repeat regions were similar between CR-1 and CR-2, and a few single nucleotide polymorphisms (SNPs) within individuals from the Russian Far East and from the Hokkaido Island were found in the first domain of CR-2 (Omote et al. 2013).

Phylogenetic relationships and divergence times between clades

The phylogenetic trees from the maximum likelihood and Bayesian analyses were identical in topology, and only the Bayesian consensus tree was shown in Fig. 2-2. Both analyses strongly supported high genetic differentiations between continental and insular clades.

The Bayesian analysis indicated that continental and insular clades diverged 670 kilo years before present (kyrBP) (95% highest posterior density interval [HPDI], 560–770 kyrBP). The timing of the most recent common ancestor for the continental clade was estimated to be 9.3 kyrBP

(95% HPDI: 1.6–20 kyrBP), and that for the insular clade was estimated to be 10 kyrBP (95% HPDI: 2.3–23 kyrBP) (Fig. 2-3). The divergence time between *B. blakistoni* and *B. flavipes* was estimated to be about 3, 500 kyrBP (95% HPDI: 3, 200–3, 700 kyrBP).

Geographical distribution of CR-2 haplotypes

Three and four CR-2 haplotypes based on nucleotide substitutions were found from the Russian Far East and Hokkaido Island, respectively. On Hokkaido Island, three of the four haplotypes were widespread, but the fourth (Fig. 2-1, yellow diamonds) was found only in eastern Hokkaido and on Kunashir Island (Fig. 2-1). The most frequent haplotype on Hokkaido (Fig. 2-1, red diamonds) was also found on Sakhalin and Kunashir Islands. In northeastern continental Asia, I newly determined haplotypes for 13 samples from Primorye, two from Amur and one from Magadan. The most common continental haplotype occurred in 12 of the 13 samples from Primorye and in the sample from Magadan, the northern boundary of the range of *B. blakistoni*. The other two haplotypes were found only in inland areas (Fig. 2-1).

Microsatellite diversity

The 22 of 34 samples obtained from the Primorye area were successfully genotyped for seven autosomal microsatellite loci reported in Omote et al. (2015). The microsatellite analysis of these samples detected no departures from Hardy-Weinberg equilibrium (P<0.05), and Ho and He in

the Primorye population were 0.64 and 0.58, respectively.

Discussion

Duplication and variation in the mitochondrial genomes

Variations of gene rearrangements in the mitochondrial genome have been reported in several avian taxa, including albatrosses, parrots, and falcons (Gibb et al. 2007). Although no rearrangements had been reported in the order Strigiformes in the present study, a gene duplication was found in *Bubo blakistoni* and *B. flavipes* that is similar to that in albatrosses (Abbott et al. 2005): there is an additional incomplete cytb gene and duplicates of ND6, $tRNA^{Thr}$, $tRNA^{Pro}$, $tRNA^{Glu}$ and CR. The rearrangements in mitochondrial genomes have occurred several times in various linages of birds. For example, Schirtzinger et al. (2012) identified six independent origins of mitochondrial CR duplications within Order Psittaciformes alone. Because the same regions in the mitochondrial genome between both *B. blakistoni* and *B. flavipes* are duplicated, this gene rearrangement could have occurred before their speciation. In the duplicated region, the differentiation between paralogous sequences within each species was smaller than that between orthologous sequences between the species, indicating the result of gene conversions. A similar pattern has been reported in some other avian lineages, such as *Amazona* parrots (Eberhard, Wright & Bermingham 2001), *Thalassarche* albatrosses (Abbott et al. 2005), and black-faced spoonbill (*Platalea minor*) (Cho et al. 2009). In several avian lineages, the paralogous sequences, which duplicated before speciation, kept

a higher similarity in each species rather than orthologous sequences, indicating that there is some system synchronizing sequences in an individual. The role of this system in the mitochondrial genome is unknown, but it is possible to prevent heteloplasmy, which is one of factors causing mitochondrial diseases.

Phylogeography of *B. blakistoni* populations

Blakiston's fish owl is classified into two subspecies, *B. b. blakistoni* on islands and *B. b. doerriesi* in the Eurasian Continent (Slaght & Surmach 2008). Although the two subspecies differ in call patterns and body markings (such as a white spot on the head in *B. b. doerriesi*), the genetic relationships between the two subspecies have not been well studied so far. The present study found two clades that were clearly separated by genetic information from the whole mitochondrial genome: one clade consisted of insular individuals (*B. b. blakistoni*) and the other of continental individuals (*B. b. doerriesi*). The genetic differences between the two clades were much higher than those within either clade, suggesting that the two geographically isolated subspecies have been separated without gene flow for a long time.

The results show that the insular and continental subspecies diverged approximately 670 kyrBP (95% HPDI: 560–770 kyrBP). Considering the data from Antarctic ice cores (Lüthi et al. 2008), these two subspecies have experienced five or six global glacial-interglacial cycles since their divergence. Because *B. blakistoni* maintains territories in forests and do not migrate to long distances, the two subspecies have remained

reproductively isolated from each other after their geographical separation. Although Sakhalin Island is located between the Eurasian Continent and Hokkaido Island, northern Sakhalin as well as the adjacent continental areas has non-forest areas that could have been a barrier to dispersal of this owl. The divergence times within the continental and insular subspecies were estimated to be approximately 9.3 and 10 kyrBP, respectively (Fig. 2-2), which were later than the end of the last glacial maximum (LGM) in 19–20 kyrBP (Clark et al. 2009). Populations of this owl would have decreased in size in the LGM due to the limited habitats and drastic changes in the environment. The low differentiation in the mitochondrial genome within the insular and continental subspecies indicates that the mtDNA haplotypes within each subspecies diverged from single mitochondrial lineages that survived the LGM. The much lower diversity of mtDNA sequences in the continental subspecies suggests an even much severe bottleneck and/or founder event. On the other hand, the nuclear microsatellite loci in the continental population showed the heterozygosity values (*Ho*: 0.64 and *He*: 0.58) roughly equivalent to those in the Hokkaido population before 1980 (*Ho*: 0.59 and *He*: 0.58), but higher than that (*Ho*: 0.51 and *He*: 0.53) in the Hokkaido population in 2005–2012 (Omote et al. 2015), which decreased in the 19th century due to human activities. Because of high mutation rates of microsatellite sequences, microsatellite analysis shows short-term demographic events. The heterozygosity values obtained in the present study suggest that the population size of the continental area was not remarkably decreased in recent years.

In continental northeastern Asia, the forest areas in the LGM were much smaller and more fragmented than those at present (Harrison et al. 2001). Blakiston's fish owls need forests and non-frozen rivers or lakes even in winter. This means that most of the continental areas, where the owls live at present, were unsuitable for them in the LGM. Refugia for the continental populations were likely located in northeastern China or Korean Peninsula, and owls likely dispersed to more northern areas after the LGM. The low variation and distribution pattern of the mtDNA haplotypes in the present continental population suggest a strong bottleneck followed by founder effect through the last glacial period. Northeastern Hokkaido, Sakhalin, and Kuril Islands could have been also unsuitable for the fish owl in the LGM. In contrast, southern Hokkaido was covered with forests (Harrison et al. 2001), and the insular population could have survived on southern Hokkaido or Honshu Island, and migrated to northeastern Hokkaido, Sakhalin and the Kuril Islands after the LGM. Since then, more variations might have been accumulated in the mtDNA and been maintained in the Hokkaido population. There are no paleontological records of Blakiston's fish owl from the Japanese islands, and future study on its past distribution is required for clarification of the migration history.

Because all of the three fish owl species phylogenetically closest to *B. blakistoni* occur in tropical forests in southern Asia (Omote et al. 2013), *B. blakistoni* is assumed to have originated in southern Asia. The divergence time between *B. blakistoni* and *B. flavipes* was estimated to be 3, 500 kyBP, or late Pliocene. During the following Pleistocene, the climate and vegetation

were repetitively changed via glacial-interglacial cycles. The ancestor of *B. blakistoni* could have adapted to colder environments during glacial periods and migrated to northeastern Asia during interglacial periods. Glacial-interglacial cycles are thought to have stimulated speciation due to geographical isolation of populations and high selective pressure for adaptation. In the case of *B. blakistoni*, the results suggest effects of climate changes on speciation. The large genetic differentiation between the continental and insular populations may lead to speciation in the future, because the two populations have not contacted each other through five or six glacial-interglacial cycles.

Chapter III

Fragmentation and low genetic diversity of the endangered Blakiston's fish owl population on Hokkaido Island

Introduction

Population genetic theory predicts that bottlenecks lead to decrease in genetic variability, individual fitness and the decreased capacity of populations to adapt to environmental change (Keller and Waller 2002). Fragmented populations may also face reduced gene flow, potentially leading to lower genetic diversity, inbreeding depression, fixation of deleterious mutations and a higher risk of extinction (Couvet 2002). A trial microsatellite analysis of the Hokkaido population of Blakiston's fish owl (120 individuals) in the intermittent intervals (1986–1993, 1997–1999 and 2009–2010) suggested diminished genetic diversity and isolation of local populations. The cause of the low level of genetic variation and gene flow was thought to be recent bottleneck; however, no genetic data showed changes of population size and structure before and after the bottleneck event assumed from field observations.

In this chapter, to clarify the temporal changes of population structure and genetic diversity in the Hokkaido population over longer period, I examined microsatellite and mitochondrial DNA (mtDNA) analyses on more current, museum and archaeological samples collected in the last century.

Material and Methods

Sampling and DNA extraction

The 439 individuals shown in Table 3-1 were used for the analyses. Total DNA was extracted from blood, tissue or cultured fibroblast samples

obtained from 405 *B. blakistoni* individuals (Table 3-1) using the DNeasy Blood & Tissue Kit (Qiagen). Most samples came from young wild owls captured at nests for banding, and the year and location of birth of these owls were known. For the last 20 years, the samples included most owls born on Hokkaido, and most wild owls injured or killed in accidents had been banded.

Blood samples were preserved in ethanol or dried on filter paper, and tissues were preserved in ethanol and frozen at -20°C until use. Fibroblasts obtained by culturing small pieces of skin tissues were frozen in liquid nitrogen until use. Total DNA was extracted from feather roots from 31 stuffed specimens (Table 3-1) using the QiaAmp DNA Micro Kit (Qiagen). The stuffed specimens had been stored in museums or research institutes, with the oldest dating from the 1880s.

In addition, using the method of Masuda et al. (2001), total DNA was extracted from three archaeological bones from different individuals, which were buried from the late 19th century to 1939 in the Nijibetsu site in the Akan area. To prevent contamination of external DNA, extraction of DNA from old samples of feathers, skins and bones was made in clean benches on different floor from the laboratory where flesh samples were used. Disposable pipette tips and microtubes were used for DNA extraction and the following experiments. The samples came from the following areas: the Ishikari Lowland, where this species is now locally extinct; the Daisetsu and Hidaka Mountains; the Akan and Konsen areas; and the Shiretoko Peninsula (Fig. 3-1). The interval used for partition data in statistical

analysis was 8 or 16 years; this corresponds to the average generation or the life span of the Blakiston's fish owl.

Analysis of mtDNA sequences

From among samples, for which familial information was available, one of sibs from each family was selected per sampling interval for analyses of mtDNA, which is maternally inherited. Part of the first domain of mtDNA control region (590 bp) was amplified and sequenced from modern samples excluding sibs (n = 113) and museum and archaeological samples (n = 34).

DNA was amplified by PCR with primers reported in Omote et al. (2013) or newly designed (Table 3-2). For analysis of old samples from museums, I designed new PCR primers to amplify three shorter fragments (78–148 bp) of the mtDNA control region. The PCRs for the museum samples were performed in a volume of 20 µl , each containing 10 µl of 2 × Multiplex PCR Master Mix (Qiagen), 4.6 µl of double-distilled water, 2.0 µl of each primer solution (2 pmol/ml), 1.0 µl of DNA template and 0.4 µl of bovine serum albumin (20 mg/ml); cycling conditions were 95°C for 15 min; 30 cycles of 94°C for 30 sec, 57°C for 3 min, and 72°C for 30 sec; and 72°C for 10 min. The PCR products were purified with the QIAquick PCR Purification Kit (Qiagen) and used as templates for nucleotide sequencing. Sequencing was performed with the BigDye Terminator v1.1 Cycle Sequencing Kit and an ABI 3130 or 3730 DNA automated sequencer (Applied Biosystems). On each of museum and archaeological samples, PCR and sequencing were performed at least three times to eliminate the potential for contamination and

sequencing errors, and confirmed the authenticity of data.

Nucleotide sequences were aligned by using MEGA 5.0 software (Tamura et al. 2011). Haplotype diversity (h) and nucleotide diversity (π) were calculated using ARLEQUIN 3.5.1.2 software (Excoffier et al. 2010). Genetic differences (Fst) among local populations (Ishikari, Daisetu, Hidaka, Akan, Konsen and Shiretoko) on Hokkaido Island (Fig. 3-1) were calculated by analysis of molecular variance (AMOVA) implemented, and tested with 10,000 permutations by using ARLEQUIN.

Analysis of microsatellite genotypes

The 407 samples of bloods, tissues, cultured fibroblasts and feathers were genotyped for seven autosomal microsatellite loci. Microsatellite markers designed for other owl species were cited: Oe058, Oe128, and Oe129 (Hsu et al. 2003, 2006); 13D8 and 4E10.2 (Thode et al. 2002); and FEPO5 and FEPO43 (Proudfoot et al. 2005). Forward primers were fluorescently labeled with 6-FAM, NED, PET, or VIC. The molecular size of PCR products was determined on an ABI 3730 DNA automated sequencer using the GS600 LIZ size standard and GENEMAPPER 4.0 software (Applied Biosystems).

Departures from Hardy-Weinberg equilibrium (HWE) and linkage disequilibrium (LD) were tested for each microsatellite locus by using ARLEQUIN. The observed (Ho) and expected (He) heterozygosities were calculated by using ARLEQUIN. Allelic richness (Ar) and inbreeding coefficient ($F$is) were calculated with FSTAT 2.9.3 software (Goudet 2001). Changes among sampling periods of Ho, He, Ar and $F$is values were tested

by pairwise non-parametric Wilcoxon signed-rank test by using STATISTICA 10 software (StatSoft). Because the sample size in older periods were small, *F*st values among local populations were calculated for each locus and combined by jackknifing, providing confidence intervals via bootstrapping, using FSTAT, and tested with 10,000 permutations by using ARLQUIN.

Effective population size (*N*e) was estimated by moment method, the bias-corrected version of the method based on LD (Waples & Do 2010), and temporal method using moment biased F-statistics (Jorde & Ryman 2007) by using NeEstimater 2.01 software (Do et al. 2014). On the moment method, *N*e was estimated on each sampling period with monogamous mating model. On the temporal method, *N*e was estimated between continuous two sampling periods, assuming that generation time was five to ten years and that census size was 100 to 150.

Populations that have undergone a bottleneck often exhibit a reduction in allele number and *H*o, with allele number decreasing faster than *H*o (Luikart & Cornuet 1999). Thus, after a bottleneck, *H*o is larger than *H*e estimated from allele frequencies assuming mutation-drift equilibrium (Cornuet & Luikart 1996). Based on this effect called heterozygosity excesses, whether a population bottleneck had occurred was tested with BOTTLENECK 1.2.0.2 software (Cornuet & Luikart 1996; Piry et al. 1999). To identify heterozygosity excesses, the Wilcoxon signed-rank test was used in default settings under three mutation models: infinite alleles (IAM), two-phased (TPM) and stepwise mutation (SMM).

To determine the number of genetic clusters that best fit the

microsatellite data, a Bayesian assignment analysis was performed with STRUCTURE 2.3 software (Pritchard et al. 2000; Falush et al. 2003). The STRUCTURE program groups multilocus data into *K* clusters without considering population origin. The STRUCTURE analysis was run for 100,000 iterations after a burn-in of 50,000 iterations, using the admixture model, and posterior probabilities were estimated for $K = 1$ through $K = 7$. For each value of *K*, 10 independent runs were conducted to quantify the amount of variation in the likelihood value for *K*. To determine the probable number of clusters, ΔK was calculated (Evanno et al. 2005). Each 10 replicate STRUCTURE runs were aligned by using CRUMPP software (Jakobsson & Rosenberg 2007). Changes in *H*o for the next 50 years were simulated based on the latest genotype data in the 2005–2012 interval by using BOTTLESIM 2.6.1 software (Kuo & Janzen et al. 2003). A single population without barrier against random mating (*N*e = 40) or completely isolated five local populations in equal sizes (*N*e = 8) were assumed. The *N*e values were based on the estimation by moment and temporal methods in the latest interval. For estimates, 1000 iterations were performed with the following constant parameters: mean life span = 16 years; age at maturity = 2 years; completely overlapping generations; each female mates with a single male each year; and sex ratio = 1:1.

Results

Variation and distribution of mtDNA haplotypes

Part of the mtDNA control region (590 bp) was sequenced for 169

individuals, including the old museum and archaeological samples; sequences were obtained for 36 of 39 stuffed specimens and three of seven archeological bones. Based on five substitution sites, five haplotypes were detected in the Hokkaido Blakiston's fish owl population and named BFH01–05. One of the five (BFH05) occurred in samples collected before 1964, but not in any subsequent samples. Before 1964, three haplotypes (BFH01, BFH03 and BFH04) were widespread on Hokkaido (Fig. 3-1a). In the 1965–1980 and 1981–1996 intervals, most haplotypes occurred in several areas (Fig. 3-1b, c), although this owl disappeared from the Ishikari area. By contrast, in the 1997–2012 interval, most haplotypes except for BFH01 were more restricted in distribution (Fig. 3-1d), and the haplotype frequencies had markedly changed. In the pre-1964 and 1965–1980 intervals, AMOVA for the haplotype data detected no genetic differences among the populations on Hokkaido (Table 3-3). After 1981, however, *F*st values among the populations were significantly high (Table 3-4). Changes of *h* and π showed similar trends (Table 3-3). In the overall Hokkaido population, both values slightly declined without significance; however, these in the local populations significantly decreased from pre-1964 to 1997–2012 intervals.

Diversity and population structure indicated by microsatellite analysis

Most individuals (99.6%, 405/407 samples) for the seven microsatellite loci examined were genotyped using blood, frozen tissue, or fibroblast samples. Attempts to amplify the microsatellite loci from old museum samples were unsuccessful. When all samples from the Hokkaido

population were analyzed as a single group, five and six of the seven loci significantly departed from HWE in the samples from 1981–1996 and 1997–2012, respectively. By contrast, less than two loci departed from HWE in each local population, excluding the Tokachi subpopulation in the 1997–2012 interval (four of the seven loci). The loci departing from HWE were different among samples from each area and period. The significant LD was detected in 0 to 14 pairs of markers, but the pairs were not common among samples from each area and period. Figure 3-2 shows estimated *N*e values by the moment method on each period and temporal method assuming that the generation time was eight years and that the census population size was 100. Both methods indicated that *N*e values were 20 to 50 in the last 20 years, *N*e was lowest in the 1980s about 10 at most 20, and the moment method suggested a remarkably large value in the oldest period 1965–1980.

The STRUCTURE analysis showed $K = 4$ to have the highest ΔK value. The four clusters corresponded mostly to the local populations on Hokkaido (Fig. 3-3). Before 1980, AMOVA for the microsatellite data detected no significant genetic differences among those local populations, but in the post-1980 intervals, *F*st values among the local populations were generally high and statistically significant (Table 3-4). Most individuals from the 1981–1996 interval were assigned only to clusters unique to local populations. In the pre-1980 and 1997–2012 intervals, however, some individuals were assigned to clusters predominantly representing other local populations, or not clearly assigned (Fig. 3-3). Mean values of *A*r were significantly decreased from the 1965–1980 interval to the 1997–2012

interval in overall Hokkaido population. Although *H*e was slightly declined, *H*o was significantly decreased more rapidly than *H*e from the 1981–1996 interval to the 1997–2012 interval (Table 3-3). By contrast, *H*o was often higher than *H*e in local populations after 1980, and Wilcoxon signed-rank tests showed significant heterozygosity excess under all three models (IAM, TPM, and SMM) in two of four local populations in the 1981–1996 interval and in two of five in the 1997–2012 interval. *F*is values were significantly increased from the pre-1980 to the 1997–2012 interval (Table 3-3). Simulations were used to predict changes in *H*o over the next 50 years, under two different assumptions: random mating occurs across the overall Hokkaido population, or the five local populations are completely isolated. The simulations under the respective assumptions predicted that *H*o would decrease to 0.44 and 0.28, respectively (86.5% and 56.2% of the values in the 2005–2012 interval).

Discussion

Temporal changes in the population structure

A trial microsatellite analysis of Blakiston's fish owls on Hokkaido in the intermittent intervals suggested that the local populations had been genetically isolated in each area. But it was not directly shown whether the local populations have been originally isolated or recently divided. To reveal this question, the present study analyzed a large number of samples (439 individuals), including samples collected before the population decline, by using mtDNA haplotype and microsatellite markers.

Before 1964, most mtDNA haplotypes were distributed over large areas of Hokkaido (Fig. 3-1), but subsequently became restricted in distribution; haplotypes BFH05, found only in a museum sample, was probably lost before 1964 (Fig. 3-1b and 3-1c). All haplotypes except BFH01 were limited to one or two areas in the 1997–2012 interval (Fig. 3-1d). AMOVA for both the mtDNA haplotype and microsatellite data detected no genetic differentiation among populations in different areas before 1964 and in the 1965–1980 interval (Table 3-3). These results indicate that gene flow occurred across large areas of Hokkaido before 1980. Among-population *F*st values from both the mtDNA haplotype and microsatellite data markedly increased after the 1980s (Fig. 3-3), suggesting major changes in the frequencies of mtDNA haplotypes due to the separation and isolation of local populations. Departures from HWE were detected for the overall Hokkaido population in the 1981–1996 and 1997–2012 intervals, and this phenomenon is known as Wahlund effect and suggests the separation and isolation of the local populations. Because marker pairs detecting LD were not common, it could have been caused by biased mating rather than links of loci. Heterozygosity excess in some local populations after 1981 also indicated a recent bottleneck in the local areas. The results suggest that the fragmentation of the owl population and subsequent reduction in population size have occurred recently on Hokkaido, probably around 1980 judging from the *F*st values (Table 3-3). Field researches observed that the population size on Hokkaido Island was minimized in the 1970s to 1980s (Brazil & Yamamoto 1989; Takenaka 1998). Actually the change of *N*e estimated from

microsatellite data also supported the bottleneck event around the 1980s (Fig. 3-2). Therefore, the population fragmentation occurred at almost the same time with the recent bottleneck. Human activities such as cultivation, housing, and building roads and dams destroy forest and river environments, and must have caused population fragmentation and bottleneck. The Blakiston's fish owl population would have been decreased and fragmented due to loss and division of habitats via vigorous human activities around the 1980s on Hokkaido.

The STRUCTURE analysis showed the optimal number of genetic clusters in Blakiston's fish owls on Hokkaido to be four; the clusters mainly correspond to the local populations. Although individuals from the Hidaka and Akan areas belonged to the same cluster, the pairwise *F*st value between the two local populations was significantly higher. The Hidaka population would have been isolated rather than interacted with the Akan population, and the small sample size in the Hidaka population probably caused the STRUCTURE result. The 1981–1996 interval was unique in that the Daisetu, Akan, and Konsen populations were each genetically uniform. In the 1997–2012 interval, some individuals were assigned to clusters that had not previously been detected in their local populations, especially in Daisetsu (Fig. 3-3), suggesting gene flow among local populations, and in fact a few owls were observed in the field to have moved from Akan and Shiretoko to Daisetsu and to have bred there in 1990 and 2002 (T. Takenaka, unpublished data). In addition, the mtDNA haplotype diversity and microsatellite diversity have increased in Daisetsu from 1981–1996 to 1997–2012 intervals,

and the lower pairwise *F*st value between Daisetsu and Shiretoko (Table 3-4) and significant departure from HWE in Daisetsu might have been caused by the migration. Due to the small population size and long life span of Blakiston's fish owl, these movements of a few individuals among local populations may have strongly affected the population structure and genetic diversity.

Temporal changes of genetic diversity in the populations

Populations that undergo bottlenecks often lose genetic diversity (Bellinger et al. 2003). Based on research on many threatened birds, Heber & Briskie (2010) concluded that population bottlenecks increase hatching failure due to inbreeding and the consequent loss of genetic diversity, particularly when the population experiences a severe bottleneck to fewer than 100–150 individuals. Changes in genetic diversity have been reported in several avian species, for which samples were analyzed before and after a bottleneck. A microsatellite analysis of the endangered black-capped vireo (*Vireo atricapilla*), which apparently experienced a bottleneck early in the 20th century, showed lower genetic diversity and increased differentiation in recent (2005–2008) samples than in historical (1899–1915) samples (Athrey et al. 2012). The great prairie-chicken (*Tympanuchus cupido*) in Wisconsin, which decreased in number by 91% via loss and fragmentation of the habitat, lost genetic diversity for both mtDNA and microsatellite markers over a period of 50 years (Johnson et al. 2004). Other studies, however, have documented no changes of genetic diversity in populations that experienced

bottleneck events. For example, the white-tail eagle (*Haliaeetus albicilla*) populations in Europe experienced dramatic declines during the 20th century, but have retained high levels of genetic diversity probably because of long generation time (average life span is around 17 years) (Hailer et al. 2006). Spanish imperial eagle (*Aquila adalberti*), of which population fragmented into small patches, reduced haplotype diversity and nucleotide diversity of mtDMA, but a microsatellite analysis showed undiminished level of nuclear diversity (Martinez et al. 2007).

Blakiston's fish owl also has a long generation time, and the present study indicated that the Hokkaido population experienced bottleneck and fragmentation event around 1980s. Although species that have a long generation time are hard to lose their nuclear diversity as reported by Hailer et al. (2006) and Martinez et al. (2007), the results showed the loss of a few alleles after the recent bottleneck and significant decrease in *A*r and *H*o (Table 3-3). This indicates a severe bottleneck, and *N*e value of the Hokkaido population around 1980 (Fig. 3-2) was actually lower than *N*e values reported by Athrey et al. (2012) and Johnson et al. (2004) in populations during bottlenecks. Generally, bottleneck events reduce heterozygosity via loss of alleles, and make *H*e smaller than *H*o (Cornuet & Luikart 1996). Heterozygosity excesses were observed in some local populations (Akan, Konsen and Daisetsu), indicating a decline of the population size in each local area. However, *H*o was decreased more rapidly than *H*e in the overall Hokkaido population. So, this could have caused biased mating. Population fragmentation could explain these results in the present study because it

restricts random mating among areas and cuts a population into tinier local patches. The *F*is values increasing after 1981 (Table 3-3) indicate a higher level of inbreeding. The mean of haplotype diversity on local populations was significantly decreased much faster than haplotype diversity on the overall Hokkaido population (Table 3-3). The results also support recent fragmentation of the Blakiston's fish owl population. Both researches on white-tail eagle and Spanish imperial eagle reported undiminished level of nuclear diversity and decline of mtDNA diversity (Hailer et al. 2006; Martinez et al. 2007). Because *N*e of the mitochondrial genome is four times lower, mtDNA haplotype diversity would be more sensitive for demographic events than nuclear diversity. The present study showed the level of genetic diversity similar to the two eagle species, but *H*o and *F*is were significantly changed. Therefore, it indicates that the Blakiston's fish owl population on Hokkaido would have undergone more serious fragmentation and inbreeding.

Inbreeding often significantly affects birth weight, survival, reproduction, and resistance to factors such as disease, predation and environmental stress (Keller and Waller 2002). The hatching rate of Blakiston's fish owl was about 20% in 2010–2013 (T. Takenaka, unpublished data), although it is still unclear whether the low rate is caused by inbreeding depression, poor food supply, aging parents or something else. For conservation of species, I need to consider genetic factors as well as ecological factors. The present study demonstrated that the genetic diversity in local populations was decreased for the last 30 years due to population

fragmentation, and that even a few movements among local populations could counter the decline in genetic diversity in Blakiston's fish owls. Simulations of changes in *H*o for the next 50 years indicated a more rapid decrease in genetic diversity when the local populations remain isolated. Therefore, conserving appropriate habitats for reproduction and promoting movements among local populations will be critical for the survival of populations and the species. Because this species has an ability to move among areas on Hokkaido as shown in the present study, their moving should be supported and promoted by conservation projects such as corridors connecting isolated habitats. For long-term conservation management of Blakiston's fish owls on Hokkaido, it is necessary to monitor changes in genetic diversity and study the movement of individual owls in the field.

Chapter IV

Duplication and variation of the major histocompatibility complex genes in Blakiston's fish owl

Introduction

The major histocompatibility complex (MHC) is a polymorphic genomic region that contains many genes, and plays a role in the adaptive immune system of jawed vertebrates. In case of human, the MHC has large and complex genomic structures, and consists of over 200 genes including class I, II and III gene families (The MHC sequencing consortium 1999). The MHC class I (MHCI) genes encode cell surface receptors to present antigen peptides for pathogens from the cytoplasm or nucleus. The MHC class II (MHCII), which consists of α and ß chains, expresses on a subset of cells such as B cells and macrophages to present antigen peptides for pathogens in intracellular vesicles and extracellular spaces. In avian species, the best characterized MHC organization is that of chicken (*Gallus gallus*). The chicken MHC possesses a highly streamlined MHC organization that contains only 19 genes including two class I and two class IIß genes (Kaufman et al. 1999). By contrast, the Japanese quail (*Coturix japonica*) MHC has a similar overall organization to the *G. gallus* MHC but differs in the number of duplicated genes with seven class I and 10 class IIß genes (Shiina et al. 2004). More complex MHC organization, which highly duplicated MHC genes, were found on several songbirds, which are the most diverse group of bird and included in landbirds clade with a variety of birds groups such as parrots, falcons, raptors, woodpeckers, and owls. In the great reed warbler (*Acrocephalus arundinaceus*), Westerdahl et al. (2000) found seven different sequences in exon 3 of MHCI and seven diverged sequences at peptide binding region of MHCIIß per individual, and suggested that the

class I and class IIß restriction fragments were linked. The zebra finch (*Taeniopygia guttata*) has highly duplicated MHCI and MHCIIß genes, which were fragmented and located on as many as four chromosomes (Balakrishnan et al. 2010). By contrast, the chicken MHC genes were located on only a micro-chromosome. This indicates that the gene fission and fusion related to chromosome rearrangements plays an important role in the evolution of complex MHC organization in passerine birds. However, chromosomal studies for MHC gene duplications were reported only on gallinaceous or passerine birds.

Recently, Kohyama et al. (2015) found up to 16 different MHCIIß alleles per individual in *B. blakistoni* based on the next generation sequencing approach. This result indicates that *B. blakistoni* genome contains at least eight MHCIIß loci, which is the largest number of gene copies reported in non-passerine birds. It is expected that the great number of MHCIIß genes in *B. blakistoni* has derived from recent gene duplication events. However, the sequencing-based approach is insufficient to reveal the accurate number of gene copies and gene structures on chromosomal level.

In this chapter, the purposes are to (1) estimate loci numbers of MHCI and MHCIIß genes, (2) observe the location of the loci on chromosomes, (3) analyze the molecular phylogenetic relationships among the alleles, and (4) discuss evolutionary patterns and variations of the MHC genes in *B. blakistoni* and closely related species.

Materials and Methods

RNA and DNA extraction

The samples for RNA extraction were obtained from two individuals of *B. blakistoni* and eagle owl (*B. bubo*), and one individual of Ural owl (*Strix uralensis*). Blood samples were stocked with heparin as anticoagulant, and precipitated at 4˚C within 12 hours since sampling. Lymphocytes were isolated from the fresh blood and cultured at 39˚C for 72 hours with 5% CO_2 in medium RPMI1640 supplemented with 20% fetal bovine serum (FBS), 90 μg/ml of phytohemagglutinin, 3 μg/ml of concanavalin A and 10 μg/ml of lipopolysaccharide as mitogens. The RNA extraction was performed with the RNeasy Plus Mini Kit (Qiagen). The extracted RNA samples were stored at -80˚C until use.

The samples for genomic DNA extraction were obtained from five individuals of *B. blakistoni*, two individuals of *B. bubo*, great horned owl (*B. virginianus*), snowy owl (*B. scandiacus*), and one individual of tawny fish owl (*B. flavipes*) and *S. uralensis*. The DNA extraction was performed with the DNeasy Blood & Tissue Kit (Qiagen).

Sequencing of the MHC class I and II genes

To determine long length sequences of RNA transcripts of MHCI and MHCII genes, complimentary DNA libraries from the total RNA of *B. blakistoni*, *B. bubo* and *S. uralensis* were synthesized by reverse transcription with the 3′-Full RACE Core Set (TaKaRa). The target genes were amplified by PCR using unique forward primers and a common reverse primer, 3′-site adaptor primer (3′-Full RACE Core Set), using PrimeSTAR

GXL DNA Polymerase (TaKaRa). The forward primer, MHCI-ex2F (5′-CGC TAC AAC CAG ASC RRS G-3′) (Alcaide et al. 2008), was used for amplifying MHC class I alleles, and the forward primers, AvesEx1-F1 (5′-ACT GGT GGC ACT GGT GGY GC-3′) and AvesEx1-F2 (5′-GCA CTG GTG GYG CTG GGA GC-3′) (Burri et al. 2014), were used for semi-nested PCR to amplify MHCIIß alleles. The PCR products were subjected to agarose-gel electrophoresis and visualized by ethidium bromide staining under an ultraviolet illumination, and candidate bands were excised and purified with the QIAEX II Gel Extraction Kit (Qiagen). Purified PCR products were cloned into the plasmid vector pBluescript II SK (+) and then transformed into *Escherichia coli* strain DH5α. The plasmids were purified with the QIAprep Spin Miniprep Kit (Qiagen) and used as templates for Sanger sequencing. Sequencing was performed with the BigDye Terminator v3.1 Cycle Sequencing Kit and an ABI 3730 DNA automated sequencer (Applied Biosystems) using M13 forward and reverse primers. Nucleotide sequences were aligned using MEGA 5.0 software (Tamura et al. 2011).

The sequence data were referred from Kohyama et al. (2015) where partial sequences (203 bp) of the MHCIIß exon 2 were obtained from 174 individuals of *B. blakistoni* by massively parallel pyrosequencing. In addition, the sequences were obtained from one individual of *B. flavipes*, two individuals of *B. bubo*, *B. virginianus*, and *B. scandiacus* by the same method as in Kohyama et al. (2015). Briefly, pyrosequencing was performed on PCR products, which were obtained from genomic DNA of the species by using the primer set, BublIIb2F (5′-GAG TGT CAG YAC CTY RAY RG-3′) and

BublIIb2R (5′-CTT TCY TCT SCS TGA YGW AGG-3′).

To reveal the relationships among MHCIIß alleles, I reconstructed phylogenetic trees by Bayesian inference using BEAST 1.6.2 software (Drummond et al. 2006; Drummond and Rambaut 2007). Phylogenetic trees of MHCIIß alleles were reconstructed based on exon 2 and exon 3 sequences separately. The phylogenetic analysis on MHCIIß exon 2 sequences used all allele data of *B. blakistoni* (accession nos. LC007937–LC007955) from Kohyama et al. (2015). In addition, the analysis included sequences of 14 other owl species obtained from GenBank as references.

Quantifying copy numbers of MHC genes

To estimate the copy numbers of MHCI and MHCIIß genes, quantitative real-time PCR (qPCR) was used with double-strand DNA-binding dye as reporter on genomic DNA. Primer sets were designed for MHCI exon 2, MHCI-Ex2-F3 (5′-CGC AAA TCA CCA AGA GGA AG-3′) and MHCI-Ex2-R1 (5′-GCC CGT AGC TCA CGT ATT TC-3′), and for MHCIIß exon 3, MHCII-Ex3-F5 (5′-CGA GGT GAA GTG GTT CCA GA-3′) and MHCIIEx3-R1 (5′-TGG TTT CCA GCA TCA CCA G-3′), based on sequences conserved in *B. blakistoni*, *B. bubo* and *S. uralensis*. In addition, the glyceraldehyde 3-phosphate dehydrogenase (GAPDH) gene was used as reference gene, as it commonly used as a single copy gene control for the qPCR based copy number validation in avian species (Criscuolo et al. 2009). A primer set was designed for the GAPDH gene exon 3, GAPDH-F2 (5′-CCA TCA CAG CCA CAC AGA AG-3′) and GAPDH-R2 (5′-TTA GCA GCC CCA

GTA GAT GC-3′), based on sequences obtained from GenBank: *Strix aluco* (KF201575), *Taeniopygia guttata* (NM_001198610), *Falco cherrug* (XM_014287574), *Nipponia nippon* (XM_009461700), and *Gallus gallus* (V00407). The qPCRs were performed on the three genes for *B. blakistoni*, *B. flavipes*, *B. bubo*, *B. virginianus*, *B. scandiacus* and *S. uralensis*. The qPCR reactions were performed using KAPA SYBER Fast qPCR kit (Kapa Biosystems). Quantitation real-time PCRs were performed using the primer sets (MHCI, MHCIIß and GAPDH) for fourth times, respectively. The 20 μl of reaction solutions contained 1–5 ng of genomic DNA, 400 nM of a primer sets and 10 μl of KAPA SYBER FAST qPCR Master Mix. The real-time amplification was performed with 7300 Real-Time PCR System (Applied Biosystems) with the condition: 95˚C for 10 min; 40 cycles of 95˚C for 5 sec and 60˚C for 30 sec; and a following dissociation stage. To generate a reference curve to control for the amplifying efficiency, qPCR run on serial dilutions (4.8 ng, 2.4 ng, 1.2 ng, 0.6 ng, 0.3 ng and 0.15 ng of DNA per reaction).

The number of MHC genes was estimated by comparing the threshold cycles (Ct) with the GAPDH gene, an internal single gene control, measured on the same sample of DNA. The number of MHC genes were calculated by a following formula: gene number = $2^{-\Delta Ct}$ where $\Delta Ct = Ct^{target\ gene} - Ct^{control}$.

Mapping of MHC loci on chromosomes

To investigate the location *B. blakistoni* and *B. bubo* MHC genes on

chromosomes, fluorescence in situ hybridization (FISH) was performed as described in Matsuda and Chapman (1995). Cloned plasmids including sequences of MHCI (1,035–1,036 bp) and MHCIIß (990 bp) genes were picked up as proves. In addition, human rRNA gene sequences (pHr21Ab: 5.8 kbp, pHr14E3: 7.3 kbp) provided from the Japanese Cancer Research Resource Bank, Japan, was used because 18S and 28S rRNAs are located closely together with MHC genes on the same micro-chromosome in some avian species such as chicken (Delany et al. 2009) and turkey (Chaves et al. 2007). Each probe was labeled with the Nick Translation Kit (Roche Applied Science) using Cy3-dUTP, and ethanol precipitated with salmon sperm DNA and *E. coli* tRNA.

Single color fluorescence in situ hybridization mapping for three types of probes was performed on the same chromosome samples by triplicate hybridization and washing in the following order: MHCIIß, MHCI, and 18S/28S rRNAs. The slides of the chromosome samples were prepared from cultured fibroblasts of *B. blakistoni* and *B. bubo*. After FISH, the slides were washed with 3:1 methanol/acetic acid, rinsed in distilled water and air-dried. The chromosomal locations of the genes were examined on the same metaphase spreads for each FISH.

Results

Sequences and phylogeny of the MHC alleles

In MHCI genes, one allele was found from more than 10 clones in both of *B. blakistoni* and *B. bubo*. Some sequence variations were also found

from both species, but the possibility could not be denied that these sequences are caused by errors occurred during PCR and/or sequencing, as it was found from only a single clone. In MHCIIß, more than 10 alleles were found from multiple clones of both *B. blakistoni* and *B. bubo* sequences. In owl species, two distinct lineages of MHCIIß alleles, DAB1 and DAB2, were defined based on exon 3 sequences (Burri et al. 2014). These two allelic lineages were found from the sequences obtained in the present study.

The Bayesian tree of MHCIIß alleles based on exon 3 sequences (Fig. 4-1) showed that DAB1 and DAB2 alleles were clearly separated in Strigidae species, while those of barn owl (*Tyto alba*) in Tytonidae consisted of an independent clade. The phylogenetic reconstruction based on MHCIIß exon 2 sequences (Fig. 4-2) also revealed that the DAB1 and DAB2 alleles of *T. alba* consisted of an independent clade. In the Strigidae clade, however, alleles in one species are most closely related to alleles in other species, rather than grouping by species. Since the most MHCIIß alleles were found by pyrosequencing based only on exon 2 sequences, it could not be determined which allelic lineages (DAB1 or DAB2) these alleles belong. Nevertheless, the alleles of which allelic lineages are known showed that DAB1 and DAB2 alleles were completely mixed in exon 2 sequences. Alleles of *B. blakistoni* were assigned into many clades together with those of Strigidae species especially *B. flavipes*.

Numbers of the MHC loci

The Ct values (Ct^{MHCI}, $Ct^{MHCIIß}$, and $Ct^{control}$) obtained by qPCR

varied only slightly among replicates from the same sample. Thus, mean Ct values were used to estimate the loci numbers. The qPCR results indicated that the number of MHCI genes was two to four: $2^{-\Delta Ct}$ = 3.9 in *B. blakistoni*, 2.0 in *B. flavipes*, 2.6 in *B. bubo*, 3.7 in *B. virginianus*, 3.7 in *B. scandiacus*, and 2.1 in *S. uralensis* (Fig. 4-3). The number of MHCIIß genes was much more various among the species: $2^{-\Delta Ct}$ = 11.9 in *B. blakistoni*, 6.0 in *B. flavipes*, 4.1 in *B. bubo*, 5.9 in *B. virginianus*, 3.6 in *B. scandiacus*, and 4.1 in *S. uralensis* (Fig. 4-3). The number of genes in *B. blakistoni* was the largest for both MHCI and MHCIIß, and was twice as many as those of *B. flavipes*.

The number of alleles found from each individual by massively parallel pyrosequencing on MHCIIß exon 2 was also shown in Table 4-1. The maximum numbers of alleles per individual were larger in *B. blakistoni* (16 copies) than other species: 12 copies *B. flavipes*, 7 copies in *B. bubo*, 4 copies in *B. virginianus*, and 7 copies in *B. scandiacus* (Table 4-1).

Location of the MHC genes on chromosomes

The locations of the MHCI, MHCIIß, and 18S and 28S rRNAs genes were investigated on chromosomes of *B. blakistoni* and *B. bubo*. The results of FISH mapping (Fig. 4-4) showed that the MHCI and MHCIIß loci are closely linked on the same pair of micro-chromosome in the both of the species. 18S and 28S rRNAs loci are located on a different pairs of micro-chromosomes from the MHC loci in both species (Fig. 4-4).

Discussion

Duplication patterns of MHC genes in *Bubo* species

The MHC region contains the most diverse set of coding genes in vertebrates because variations of MHC genes are necessary to recognize many types of antigens in immune responses. Chicken has the minimum essential MHC (Kaufman et al. 1999), but MHC of quail and songbirds contain much more genes (Westerdahl et al. 2000; Shiina et al. 2004; Balakrishnan et al. 2010). Most genes of the MHC family are assumed to have evolved by gene duplications. Gene duplication is mainly caused by recombination, replication slippage, retrotransposition or chromosome duplication. The number of retroelements found in quail and songbirds is high for bird but smaller than that in human, whereas there is no retroelement found in chicken (Hess et al. 2002). Balakrishnan et al. (2010) reported highly duplicated and interspersed MHC genes on many chromosomes in the zebra finch.

The present study revealed high variations in the numbers of MHCI and MHCIIß loci among *Bubo* species by qPCR-based copy number validation. The number of MHCIIß loci was more variable, and that of *B. blakistoni* (12 ± 2) was remarkably larger than the other *Bubo* species (less than six) (Fig. 4-3). The result of massively parallel pyrosequencing showed largest number of MHCIIß alleles on *B. blakistoni* (up to 16 alleles per individual). This result indicated that *B. blakistoni* has more than eight MHCIIß loci. The pyrosequencing results on the other *Bubo* species roughly corresponded with the number of MHCIIß loci estimated by qPCR (Fig. 4-3). These results indicate frequent duplication of MHCIIß loci in *Bubo* species.

The numbers of both MHCI and MHCIIß loci in *B. blakistoni* were twice as many as those in *B. flavipes*, the closest related species. This suggests duplication of MHC genes in *B. blakistoni* after speciation: probably the whole set of MHC gene family might have duplicated at one time.

To reveal the pattern of gene duplication, I investigated the location of the MHC gene loci on chromosomes of *B. blakistoni* and *B. bubo*, whose MHCI and MHCIIß loci were less than half of those of *B. blakistoni*. *Bubo blakistoni* and *B. bubo* have 82 and 84 chromosomes including micro-chromosomes, respectively. The FISH results showed that MHCI and MHCIIß loci are located in the same site on a pair of chromosomes, indicating that the duplication of MHC genes was not at chromosomal level, but tandem replication within the gene family region. It is unclear whether or not the whole MHC genes were duplicated at the same time as a group. To clarify the details of MHC gene duplication history in *B. blakistoni*, it is necessary to survey the genomic structures in the MHC region using such as BAC clone sequencing.

Variation of MHCIIß alleles in *Bubo blakistoni*

Exon 3 sequences in the DAB1 and DAB2 alleles of Strigidae species were completely separated (Fig. 4-1), indicating that the two lineages of alleles had been diverged before speciation and evolved as paralogs. But only the sequences of exon 2, which codes antigen-recognition sites, were mixed among DAB1 and DAB2 alleles (Fig. 4-2). Gene conversion among DAB1 and DAB2 alleles might have caused the rearrangements of sequences and

increase of allele variations.

The MHCIIß alleles of *B. blakistoni* were assigned into several clusters, which consist of those of Strigidae species, and nearest to those of *B. flavipes* in the most clusters (Fig. 4-2). It means that most of the MHCIIß alleles in *B. blakistoni* was derived from the common ancestor with *B. flavipes*. In general, high level of variations in MHC genes often observed in wild animals are involved in resistance to diseases, but it is difficult to maintain the variation in small populations because of the strong effect of genetic drift and inbreeding. *Bubo blakistoni* is a unique raptor hunting freshwater fish in the subarctic region, and needs large special habitats. The other fish owl species including *B. flavipes* live in tropical or subtropical regions in Eurasia. The *B. blakistoni* populations could have experienced severe bottlenecks through the glacial periods. Population bottlenecks and founder effects through glacial periods could have reduced genetic variations. In addition, the recent population fragmentation and declining owing to human activities decreased genetic variation, and the level of MHCIIß variation became low in the current *B. blakistoni* population on Hokkaido Island (Kohyama et al. 2015). But the allele number per individual was still large among owl species (Table 4-1), probably because of multiple MHCIIß loci. When the loci are duplicated, the expected number of alleles per individual could be remarkably increased. The duplication of MHC genes could have prevented declining of immunity in this tiny population and contributed to the successful range expansion of *B. blakistoni* into unstable subarctic regions.

General Discussion

Blakiston's fish owl (*Bubo blakistoni*) comprises two subspecies: *B. b. doerriesi* in continental Eurasia and *B. b. blakistoni* on Hokkaido and the southern Kuril Islands. The phylogenetic analyses based on mtDNA sequences showed that *B. blakistoni* was included in genus *Bubo* with other three fish owl species in southern Asia. The tandem repeat sequences found in mtDNA control region of fish owl species also suggest the close relationship among them. The phylogenetic analyses using all mitochondrial genes support the classification of the two subspecies in *B. blakistoni* with deep divergence time (670 kyBP). The divergence among haplotypes (about 10 kyBP) within each subspecies was estimated to have occurred after the last glacial period. Information on the paleodistribution of vegetation suggests that main areas now inhabited by *B. blakistoni* were unsuitable as habitats during the last glacial maximum. The low variations in the mitochondrial genome within the insular and continental populations indicate that severer bottlenecks and subsequent founder events occurred at least during the last glacial period.

On Hokkaido Island, *B. blakistoni* was formerly widespread, but its population size decreased during the 20th century due to reduction and fragmentation of its habitat through human activities. Populations that undergo bottlenecks often lose genetic diversity. The effective population size estimated by microsatellite analysis showed decrease of population size around the 1980s. To reveal the change of the population structure and genetic diversity, the present study analyzed a large amount of samples (442

individuals), including samples collected before the population decline, using mtDNA haplotype and microsatellite markers. Most mtDNA haplotypes were formerly distributed over large areas of Hokkaido, but subsequently became restricted in distribution. Both of the mtDNA haplotype and microsatellite data suggested no genetic differentiation among local populations before 1980, and remarkable differentiation after then. These results indicate that gene flow occurred across large areas of Hokkaido before, and that the fragmentation of the owl population and subsequent reduction in population size have happened recently. Human activities such as cultivation, housing, and building roads and dams destroy forest and river environments, and caused population fragmentation and bottleneck. Both of microsatellite and mtDNA analyses showed the loss of genetic diversity after the recent bottleneck, and inbreeding coefficient values calculated by microsatellite data indicated a higher level of inbreeding. In addition, the variations of MHC genes, which play a role in the adaptive immune system, were investigated. The results of quantitative real-time PCR and massively parallel pyrosequencing suggested that numbers of MHC class I and class IIß loci in *B. blakistoni* were larger than other owl species, indicating recent duplication of the genes. The chromosomal mapping showed that the locations of MHC class I and class IIß were closely linked on a micro-chromosomes. It means that the MHC loci were tandemly duplicated in a limited chromosome region. The gene duplication increases the variations of MHC genes in this owl species, and could have improved adaptation of tiny populations. However, the diversity of the MHC class IIß

gene has also decreased for the last thirty years in Hokkaido (Kohyama et al. 2015). The present study demonstrated that the genetic diversity in local populations was decreased due to population fragmentation, and that even a few movements among local populations could counter the decline in genetic diversity in Blakiston's fish owls. Therefore, conserving appropriate habitats for reproduction and promoting movements among local populations can be critical for the survival of populations and the species. Thus, the results obtained in the present study could very much contribute to not only basic evolutionary study of populations and species, but also the advance of conservation activities of endangered species.

Acknowledgements

I would like to thank Professor Ryuichi Masuda (Hokkaido University) for invaluable guidance and instruction through this study. I am also grateful to Professor Takeo Horiguchi (Hokkaido University), Professor Shin Tochinai (Hokkaido University), and Associate Professor Hiroshi Kajihara (Hokkaido University) for reviewing this thesis. In addition, I would like to present my thanks to Ms. Chizuko Nishida (Hokkaido University), Dr. Takeshi Takenaka (FILIN), Dr. Keisuke Saitou (Institute for Raptor Biomedicine), Dr. Yuko Hayashi (Sapporo University), and Mr. Sumio Yamamoto (Nemuro City) for kindly providing samples and suggestions. I also thank Dr. Matthew Dick for invaluable comments and editing the manuscript.

I thank the Kushiro Nature Conservation Office, Ministry of the Environment, for providing modern samples and invaluable suggestions. The samples were originally obtained through activities to conserve Blakiston's fish owls by the Ministry of the Environment, Japan. Feather samples from stuffed specimens were provided from the Yamashina Institute for Ornithology (Takeshi Yamasaki, Yasuko Iwami, and Takema Saitou), the Botanical Garden of Hokkaido University (Fumihito Takaya), Tomakomai Experimental Forest Hokkaido University (Hiroshi Sugiyama), the University of Tokyo Hokkaido Forest, the National Museum of Nature and Science Tokyo (Isao Nishiumi), Abiko City Museum of Birds (Ken-ichi Tokita), Betsukai Town Local Museum (Kazuto Ishiwata), Erimo Town Local Museum (Toshiyasu Nakaoka), Kamishihoro Town Higashitaisetsu Museum,

Kushiro City Museum, Mombetsu City Museum, Nakashibetsu Town Local Museum, Nemuro City Museum of History and Nature, Rausu Town Local Museum, Shari Town Shiretoko Museum, Sounkyo Visitor Center (Toru Katayama), Tomakomai City Museum (Aiko Kodama), Urakawa Town Local Museum, and the Shimane Prefecture Sanbe Nature Center. I am also grateful to Hiroshi Utagawa and Toshiro Kumaki (University of Tokyo) for providing archaeological bone samples.

Tissue sampling in the continental part of the species range was managed by the Amur-Ussuri Center for Avian Biodiversity in cooperation with the Wildlife Conservation Society Russia Program. Critically important samples were provided by Mr. Sergey, Surmach, Dr. Nikolai Dokuchaev, Dr. Sergei Avdeyuk and Dr. Jonathan Slaght. Export of the continental samples to Japan was done according to the CITES permit #14RU001618 of 20.10. 2014 issued by the Federal Service of Natural Resources Management of Russian Federation.

I thank the Ueno Zoological Gardens (Eri Okuyama), Matsue Vogel Park (Hideki Hashimoto), Tama Zoological Park, Sapporo Maruyama Zoo, and Kushiro City Zoo for providing samples of other owl species.

References

Abbott CL, Double MC, Trueman JWH, Robinson A, Cockburn A. 2005. An unusual source of apparent mitochondrial heteroplasmy: duplicate mitochondrial control regions in *Thalassarche albatrosses*. Molecular Ecology 14: 3605–3613

Alcaide M, Edwards SV, Cadahía L, Negro JJ. 2008. MHC class I genes of birds of prey: isolation, polymorphism and diversifying selection. Conservation Genetics 10: 1349–1355

Athrey G, Barr KR, Lance RF, Leberg PL. 2012. Birds in space and time: genetic changes accompanying anthropogenic habitat fragmentation in the endangered black-capped vireo (*Vireo atricapilla*). Evolutionary Applications 5: 540–552

Balakrishnan CN, Ekblom R, Völker M, Westerdahl H, Godinez, Kotkiewicz RH, Burt DW, Graves T, Griffin DK, Warren WC, Edwards SV. 2010. Gene duplication and fragmentation in the zebra finch major histocompatibility complex. BMC Biology 8: 29

Barrowclough, GF, Groth, JG, Mertz, LA, Gutierrez, RJ. 2005. Genetic structure, introgression, and a narrow hybrid zone between northern and California spotted owls (*Strix occidentalis*). Molecular Ecology 14: 1109–1120

The MHC sequencing consortium. 1999. Complete sequence and gene map of a human major histocompatibility complex. Nature 401: 921–923

Bellinger MR, Johnson JA, Toepfer J, Dunn P. 2003. Loss of genetic variation in greater prairie chickens following a population bottleneck in Wisconsin, U.S.A. Conservation Biology 17: 717–724

Brazil M, Yamamoto S. 1989. The distribution of owls in Japan. Raptors in the modern world. WWGB, Berlin, London and Paris. 389–401

Burri R, Promerová M, Goebel J and Fumagalli L. 2014. PCR-based isolation of multigene families: lessons from the avian MHC class IIB. Molecular Ecology 14: 778–788

Chaves LD, Krueth SB, Reed KM. 2007. Characterization of the turkey MHC chromosome through genetic and physical mapping. Cytogenetic and Genome Research 117: 213–220

Chen J-M, Cooper DN, Chuzhanova N, Férec C, Patrinos GP. 2007. Gene conversion: mechanisms, evolution, and human disease. Nature Reviews Genetics 8: 762–775

Cho HJ, Eda M, Nishida S, Yasukochi Y, Chong JR, Koike H. 2009. Tandem duplication of mitochondrial DNA in the black-faced spoonbill, *Platalea minor*. Genes & Genetic System 84: 297–305

Clark PU, Dyke AS, Shakun JD, Carlson AE, Clark J, Wohlfarth B, Mitorovica JX, Hostetler SW, McCabe AM. 2009. The Last Glacial Maximum. Science 325: 710–714

Cornuet JM, Luikart G. 1996. Description and power analysis of two tests for detecting recent population bottlenecks from allele frequency data. Genetics 144: 2001–2014

Couvet D. 2002. Deleterious effect of restricted gene flow in fragmented

populations. Conservation Biology 16: 369–376

Criscuolo F, Bize P, Nasir L, Metcalfe NB, Foote CG, Griffiths K, Gault EA, Monaghan P. 2009. Real-time quantitative PCR assay for measurement of avian telomeres. Journal of Avian Biology 40: 342–347

Delany ME, CRobinson CM, Goto RM, Miller MM. 2009. Architecture and organization of chicken microchromosome 16: Order of the *NOR*, *MHC-Y*, and *MHC-B* subregions. Journal of Heredity 100: 507–514

Do C, Waples RS, Peel D, Macbeth G M, Tillett BJ, Ovenden JR. 2014. NeEstimator v2: re-implementation of software for the estimation of contemporary effective population size (Ne) from genetic data. Molecular Ecology Resource 14: 209–214

Drummond AJ, Ho SYW, Phillips MJ, Rambaut A. 2006. Relaxed phylogenetics and dating with confidence. PLoS Biology 4: 699–710

Drummond AJ, Rambaut A. 2007. BEAST: Bayesian evolutionary analysis by sampling trees. BMC Evolutionary Biology 7: 214

Eberhard JR, Wright TF, Bermingham E. 2001. Duplication and concerted evolution of the mitochondrial control region in the parrot genus *Amazona*. Molecular Biology and Evolution 18: 1330–1342

Eo SH, DeWoody JA. 2010. Evolutionary rates of mitochondrial genomes correspond to diversification rates and to contemporary species richness in birds and reptiles. Proceeding of the Royal Society B 277: 3587–3592

Evanno G, Regnaut S, Goudet J. 2005. Detecting the number of clusters of individuals using the software STRUCTURE: a simulation study. Molecular Ecology 14: 2611–2620

Excoffier L, Lischer HEL. 2010. Arlequin suite ver 3.5: a new series of programs to perform population genetics analyses under Linux and Windows. Molecular Ecology Resources 10: 564–567

Falush D, Stephens M, Pritchard JK. 2003. Inference of population structure using multilocus genotype date: linked loci and correlated allele frequencies. Genetics 164: 1567–1587

Gibb GC, Kardailsky O, Kimball RT, Braun EL, Penny D. 2007. Mitochondrial genomes and avian phylogeny: complex characters and resolvability without explosive radiations. Molecular Biology and Evolution 24: 269–280

Goudet J. 2001. FSTAT, a program to estimate and test gene diversities and fixation indices version 2.9.3. http://www2.unil.ch/popgen/softwares/fstat.htm. Updated from Goudet (1995)

Harrison SP, Yu G, Takahara H, Prentice IC. 2001. Diversity of temperate plants in east Asia. Nature 413: 129–130

Harrison GL, McLenachan PA, Phillips MJ, Slack KE, Cooper A, Penny D. 2004. Four new avian mitochondrial genomes help get to basic evolutionary questions in the late Cretaceous. Molecular Biology and Evolution 21: 974–983

Hailer F, Helander B, Folkestad AO, Ganusevich SA, Garstad S, Hauff P, Koren C, Nygard T, Volke V, Vila C, Ellegren H. 2006. Bottleneck but long-lived: high genetic diversity retained in white-tailed eagles upon recovery from population decline. Biology Letters 2: 316–319

Hayashi Y. 1997. Home range, habitat use and natal dispersal of Blakiston's

Fish-owls. Journal of Raptor Research 31: 283–285

Hayashi Y. 1999. Past and present distribution of Blakiston's fish owl (*Ketupa blakistoni*) in Hokkaido, Japan–based upon museum specimens–. Journal of Yamashina Institute Ornithol 31: 45–61

Heber S, Briskie JV. 2010. Population bottlenecks and increased hatching failure in endangered birds. Conservation Biology 24: 1674–1678

Hess CM1, Gasper J, Hoekstra HE, Hill CE, Edwards SV. 2000. MHC class II pseudogene and genomic signature of a 32-kb cosmid in the house finch (*Carpodacus mexicanus*). Genome Research 10: 613–623

Hsu Y-C, Li S-H, Lin Y-S, Severinghaus LL. 2006. Microsatellite loci from Lanyu scops owl (*Otus elegans botelensis*) and their cross-species application in four species of Strigidae. Conservation Genetics 7:161–165

Hsu Y-C, Severinghaus LL, Lin Y-S, Li S-H. 2003. Isolation and characterization of microsatellite DNA markers from the Lanyu scops owl (*Otus elegans botelensis*). Molecular Ecology Notes 3: 595–597

Jakobsson M, Rosenberg NA. 2007. CLUMPP: a cluster matching and permutation program for dealing with label switching and multimodality in analysis of population structure. Bioinformatics 23: 1801–1806

Jobb G, von Haeseler A, Strimmer K. 2004. TREEFINDER: A powerful graphical analysis environment for molecular phylogenetics. BMC Evolutionary Biology 4: 18

Johnson JA, Bellinger MR, Toepfer JE, Dunn P. 2004. Temporal changes in allele frequencies and low effective population size in greater prairie-chickens. Molecular Ecology 13: 2617–2630.

Jorde PE, Ryman N. 2007. Unbiased estimator for genetic drift and effective population size. Genetics 177: 927–935

Kaufman J, Milne S, Göbel TW, Walker BA, Jacob JP, Auffray C, Zoorob R, Beck S. 1999. The chicken B locus is a minimal essential major histocompatibility complex. Nature 401: 923–925

Keller LF, Waller DM. 2002. Inbreeding effects in wild populations. Trends in Ecology & Evolution 17: 230–241

Kohyama TI, Omote K, Nishida C, Takenaka T, Saito K, Fujimoto S, Masuda R. 2015. Spatial and temporal variation at major histocompatibility complex class IIB genes in the endangered Blakiston's fish owl. Zoological Letters 1: 13

König C, Weick W. 2008. Owls. A Guide to the Owls of the World, second ed. Christopher Helm, London

Kuo CH, Janzen FJ. 2003. BOTTLESIM: a bottleneck simulation program for long-lived species with overlapping generations. Molecular Ecology Notes 3: 669–673

Luikart G, Cornuet JM. 1999. Estimating the effective number of breeders from heterozygote excess in progeny. Genetics 151: 1211–1216

Lüthi D, Floch ML, Bereiter B, Blunier T, Barnola J-M, Siegenthaler U, Raynaud D, Jouzel J, Fischer H, Kawamura K, Stocker TF. 2008. High-resolution carbon dioxide concentration record 650,000–800,000 years before present. Nature Letters 15: 379–382

Lunt DH, Whipple LE, Hyman BC. 1998. Mitochondrial DNA variable number tandem repeats (VNTRs): utility and problems in molecular ecology. Molecular Ecology 7: 1441–1455

Martinez BC, Godoy JA, Negro JJ. 2007. Population fragmentation leads to spatial and temporal genetic structure in the endangered Spanish imperial eagle. Molecular Ecology 16: 477–486.

Masuda R, Amano T, Ono H. 2001. Ancient DNA analysis of brown bear (*Ursus arctos*) remains from the archeological site of Rebun Island, Hokkaido, Japan. Zoological Science 18: 741–751

Matsuda Y, Chapman VM. 1995. Application of fluorescence in situ hybridization in genome analysis of the mouse. Electrophoresis 16: 261–72

Omote K, Nishida C, Dick MH, Masuda R. 2013. Limited phylogenetic distribution of a long tandem-repeat cluster in the mitochondrial control region in Bubo (Aves, Strigidae) and cluster variation in Blakiston's fish owl (*Bubo blakistoni*). Molecular Phylogenetics and Evolution 66: 889-897

Omote K, Nishida C, Takenaka T, Saito T, Shimura R, Fujimoto S, Sato T, Masuda R. 2015. Recent fragmentation of the endangered Blakiston's fish owl (*Bubo blakistoni*) population on Hokkaido Island, northern Japan, revealed by mitochondrial DNA and microsatellite analyses. Zoological Letters 1: 16

Piry S, Luikart G, Cornuet JM. 1999. BOTTLENECK: a computer program for detecting recent reductions in the effective population size using allele frequency data. Journal of Heredity 90: 502–503

Pritchard JK, Stephens M, Donnelly P. 2000. Inference of population

structure using multilocus genotype date. Genetics 155: 945–959

Proudfoot G, Honeycutt R, Slack RD. 2005. Development and characterization of microsatellite DNA primers for ferruginous pygmy-owls (*Glaucidium brasilianum*). Molecular Ecology Notes 5: 90–92

Roukonen M, Kvist L. 2002. Structure and evolution of the avian mitochondrial genome. Molecular Phylogenetics and Evolution 23: 422–432

Saccone C, Pesole G, Sbis E. 1991. The main regulatory region of mammalian mitochondrial DNA: structure-function model and evolutionary pattern. Journal of Molecular Evolution 33: 83–91

Schirtzinger EE, Tavares ES, Gonzales LA, Eberhard JR, Miyaki CY, Sanchez JJ, Hernandez A, Müeller H, Graves GR, Fleischer RC, Wright TF. 2012. Multiple independent origins of mitochondrial control region duplications in the order Psittaciformes. Molecular Phylogenetics and Evolution 64: 342–356

Shiina T, Shimizu S, Hosomichi K, Kohara S, Watanabe S, Hanzawa K, Beck S, Kulski JK, Inoko H. 2004. Comparative genomic analysis of two avian (quail and chicken) MHC regions. Journal of Immunology 172: 6751–6763

Slaght JC, Surmach SG. 2008. Biology and conservation of Blakiston's fish-owls (*Ketupa blakistoni*) in Russia: a review of the primary literature and an assessment of the secondary literature. Journal of Raptor Research 42: 29–37

Sorenson MD, Ast JC, Dimcheff DE, Tamaki Y, Mindell DP. 1999. Primers for a PCR-based approach to mitochondrial genome sequencing in birds

and other vertebrates. Molecular Phylogenetics and Evolution 12: 105–114

Swofford DL. 2002. PAUP* Phylogenetic Analysis Using Parsimony (and Other Methods) Version 4. Sinauer Associates, Sunderland

Takenaka K. 1998. Distribution, habitat environments, and reasons for reduction of the endangered Blakiston's fish owl in Hokkaido, Japan. Doctoral dissertation

Tamura K, Peterson D, Peterson N, Stecher G, Nei M, Kumar S. 2011. MEGA5: molecular evolutionary genetics analysis using maximum likelihood, evolutionary distance, and maximum parsimony methods. Molecular Biology and Evolution 28: 2731–2739

Thode AB, Maltbie M, Hansen LA, Green LD, Longmire JL. 2002. Microsatellite markers for the Mexican spotted owl (*Strix occidentalis lucida*). Molecular Ecology Notes 2: 446–448

Valverde JR, Marco R, Garesse R. 1994. A conserved heptamer motif for ribosomal RNA transcription termination in animal mitochondria. Proceeding of the National Academy of Science USA 91: 5368–5371

Waples RS, Do C. 2010. Linkage disequilibrium estimates of contemporary Ne using highly variable genetic markers: a largely untapped resource for applied conservation and evolution. Evolutionary Applications 3: 244–262

Wenink PW, Baker AJ, Tilanus MGJ. 1994. Mitochondrial control-region sequences in two shorebird species, the turnstone and the dunlin, and their utility in population genetic studies. Molecular Biology and Evolution 11: 22–31

Westerdahl H, Wittzell H, Schantz T von. 2000. MHC diversity in two

passerine birds: no evidence for a minimal essential MHC. Immunogenetics 52: 92–100

Wink M, El-Sayed A-A, Sauer-Gürth H, Gonzalez J. 2009. Molecular phylogeny of owls (Strigiformes) inferred from DNA sequences of the mitochondrial cyt *b* and the nuclear *RAG-1* gene. Ardea 97: 581–591

Xiao B, Ma F, Sun Y, Li Q-W. 2006. Comparative analysis of complete mitochondrial DNA control region of four species of Strigiformes. Acta Genetica Sinica 33: 965–974

Yamamoto S. 1999. Simahukurou. Hokkaido Shimbun Press, Sapporo (in Japanese)

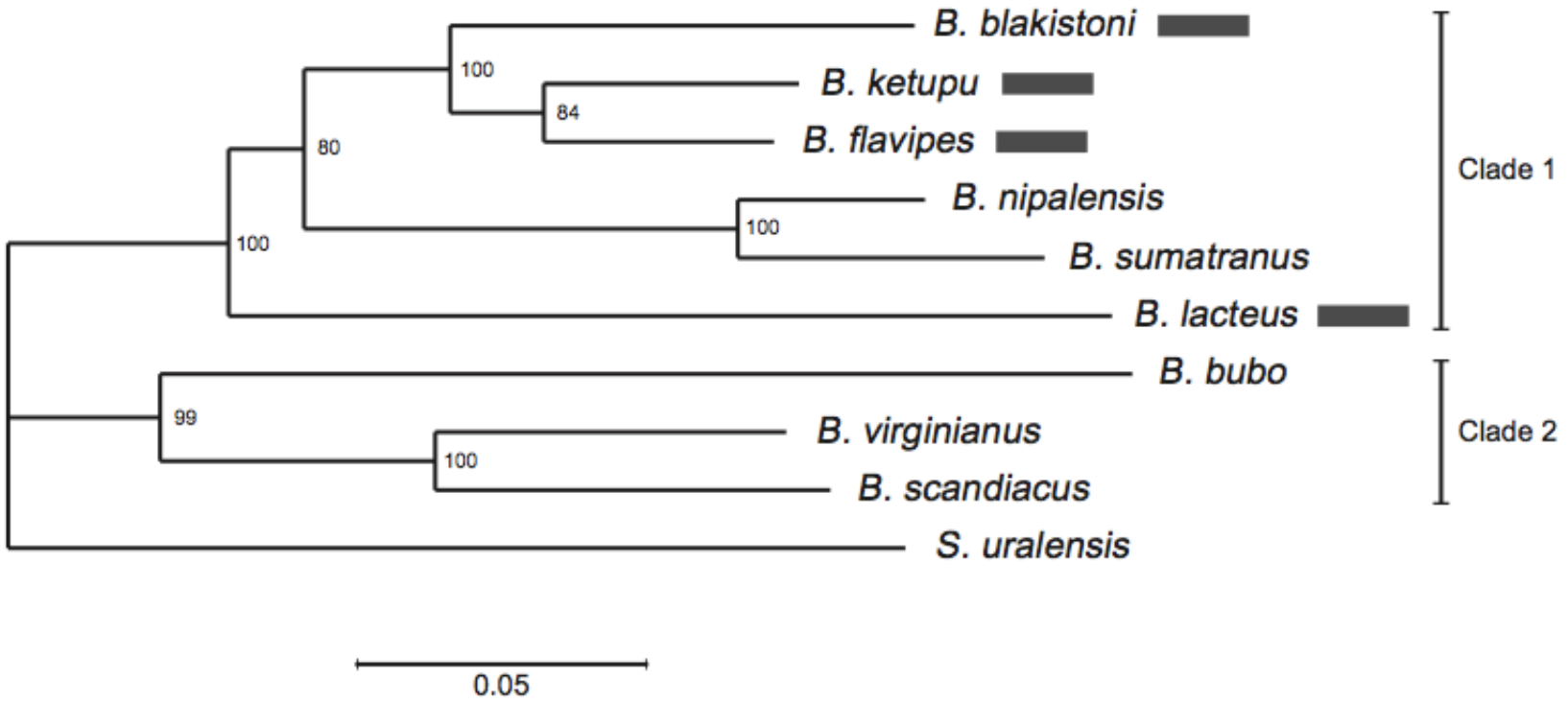

Fig. 1-1 Maximum-likelihood tree for nine *Bubo* species and the outgroup *Strix uralensis*, based on a combined analysis of mitochondrial cyt *b* (1140 bp) and control region (1282 bp) sequences from Omote et al. (2013). Numbers near nodes indicate bootstrap values derived from 1000 replicates. Thick bars indicate species that have a large cluster of tandem repeats in the mtDNA control region. The scale bar at bottom indicates substitutions per site.

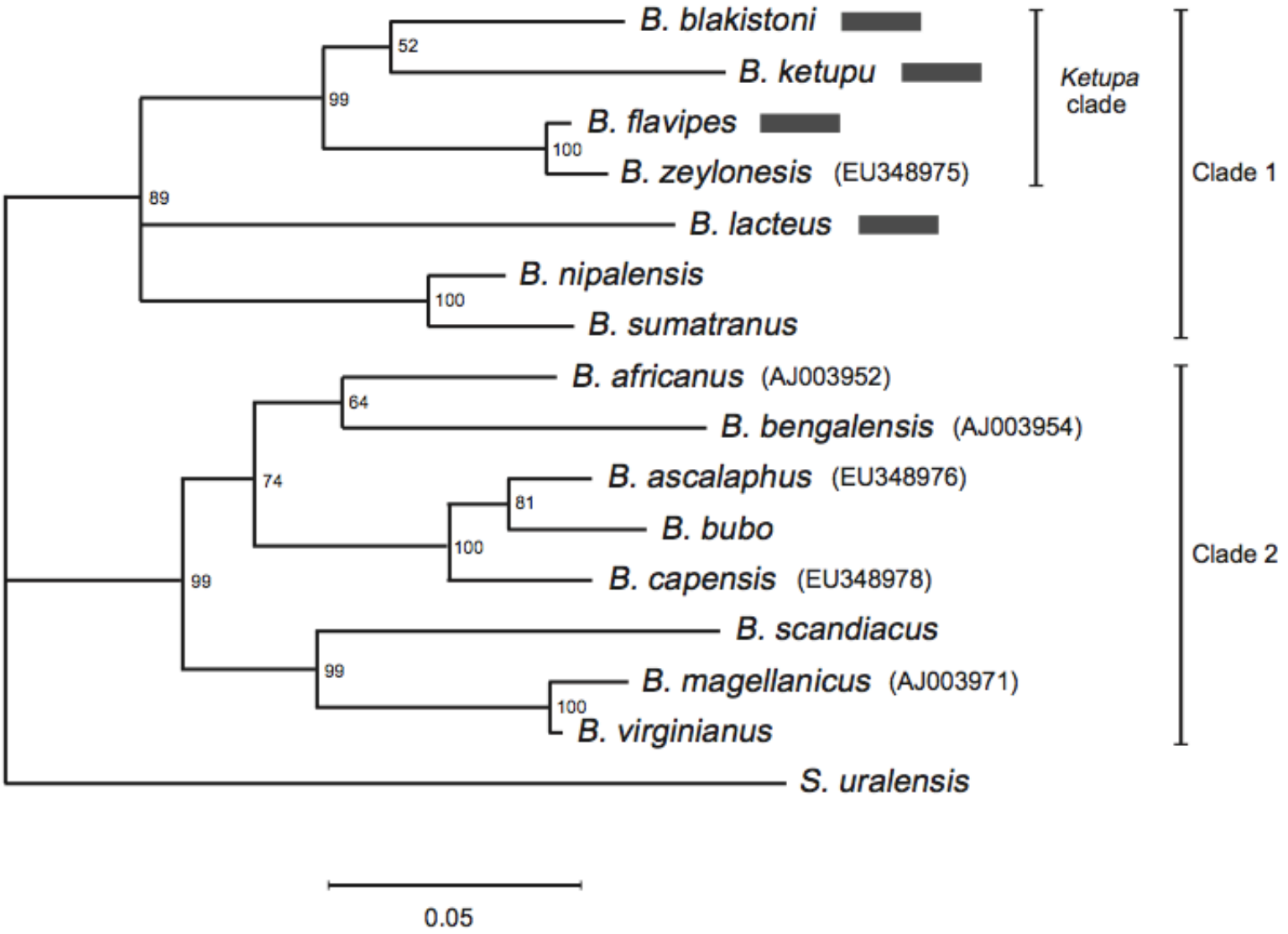

Fig. 1-2 Maximum-likelihood tree for 15 *Bubo* species and the outgroup, *Strix uralensis*, based on cyt *b* sequences (1001 bp) from Omote et al. (2013). Numbers near nodes indicate bootstrap values derived from 1000 replicates. Thick bars indicate species that have a large cluster of tandem repeats in the mtDNA control region. The scale bar at bottom indicates substitutions per site.

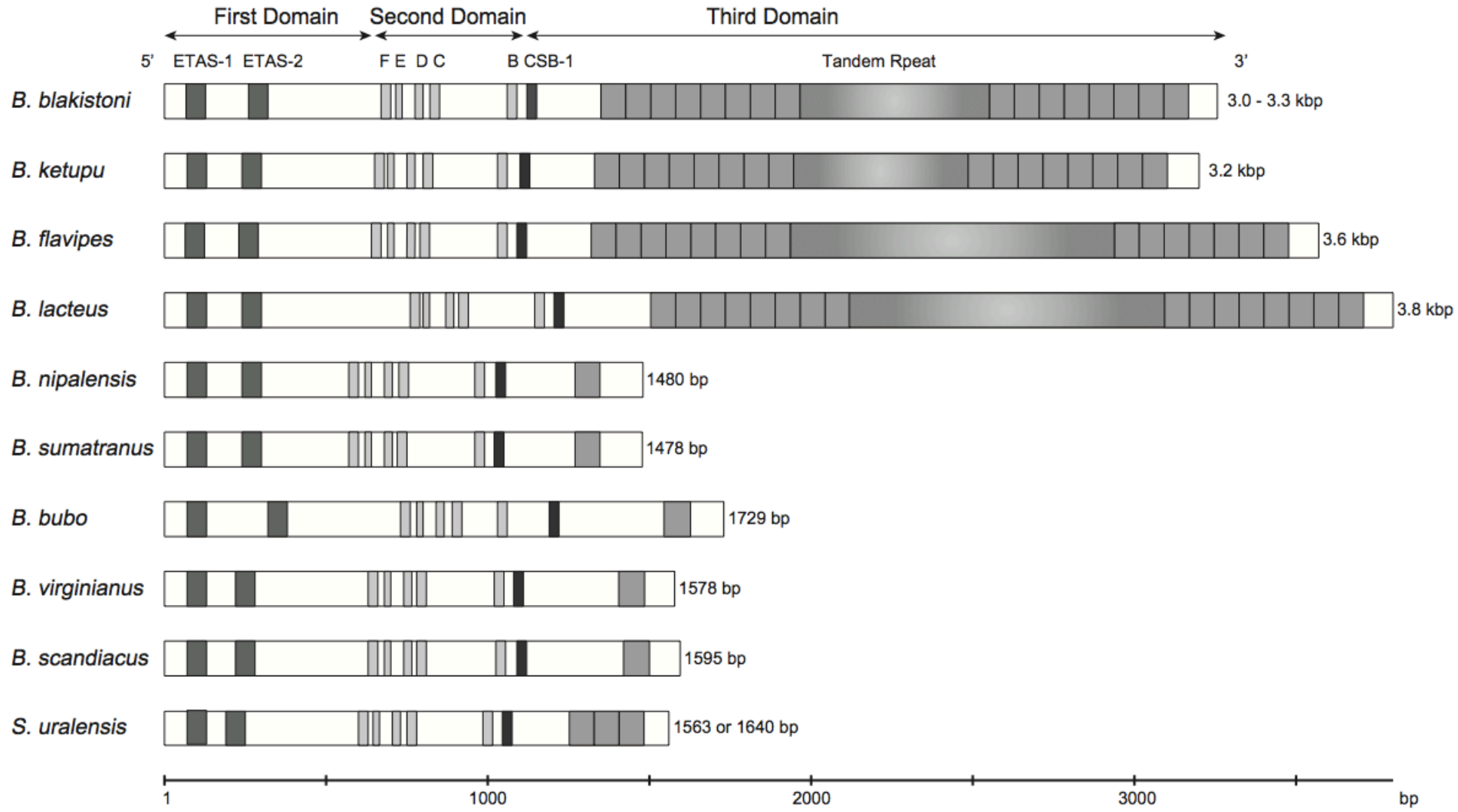

Fig. 1-3 Molecular organization of the complete mtDNA control region in nine *Bubo* species and *Strix uralensis*.from Omote et al. (2013).

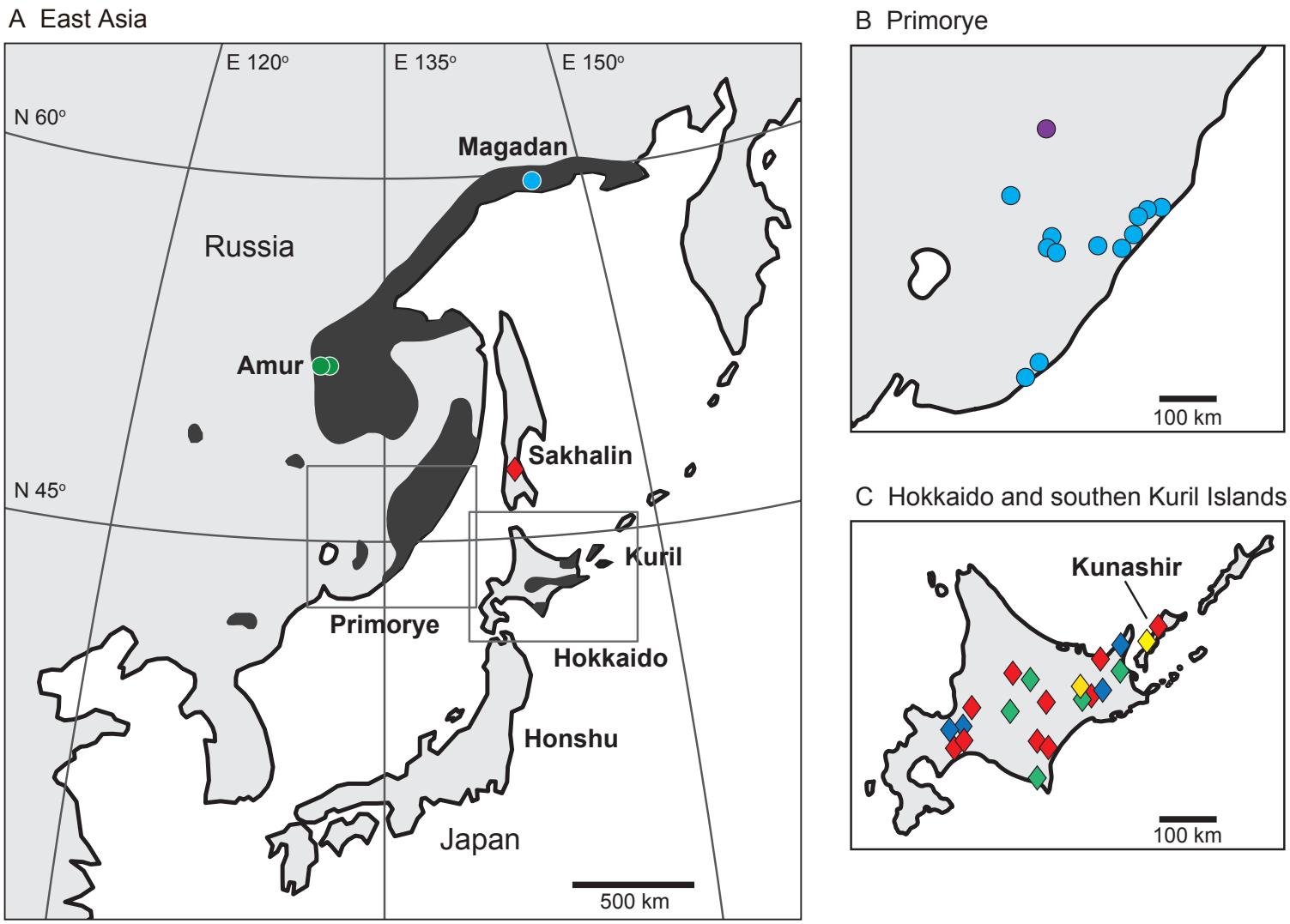

Fig. 2-1 Geographical distribution (dark gray) of Blakiston's fish owl (*Bubo blakistoni*) and the distribution of mtDNA haplotypes in Northeast Asia (A), Prymorye (B) and Hokkaido and southern Kuril (C). Circles, mtDNA haplotypes in the continental clade; diamonds, mtDNA haplotypes in the insular clade (cited from Omote *et al*., 2015); each color refers to a different mtDNA CR-2 haplotype based on nucleotide sequences.

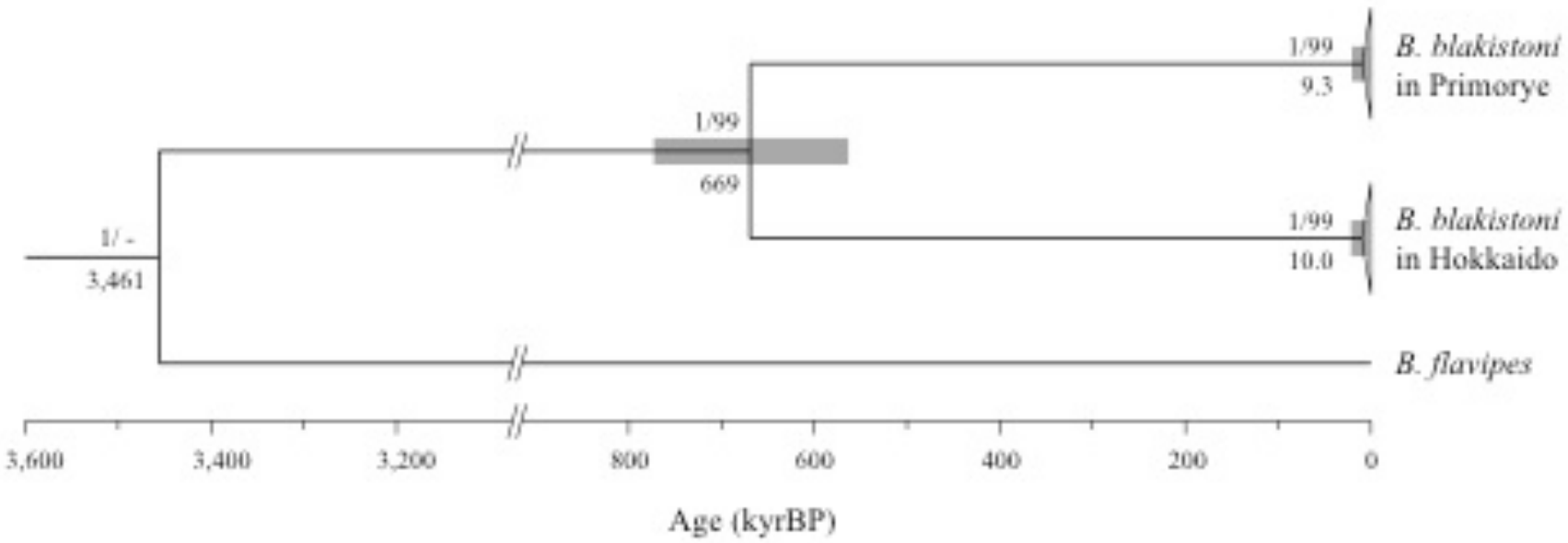

Fig. 2-2 The molecular phylogeny based on the whole mitochondrial genome sequences of *Bubo blakistoni* and *B. flavipes* as an out-group. Numbers above the three branches indicate the Bayesian posterior probabilities / ML bootstrap values. Numbers below branches show the estimated divergence times, and the bars mean 95% HPD intervals. kyrBP, kiro years before present.

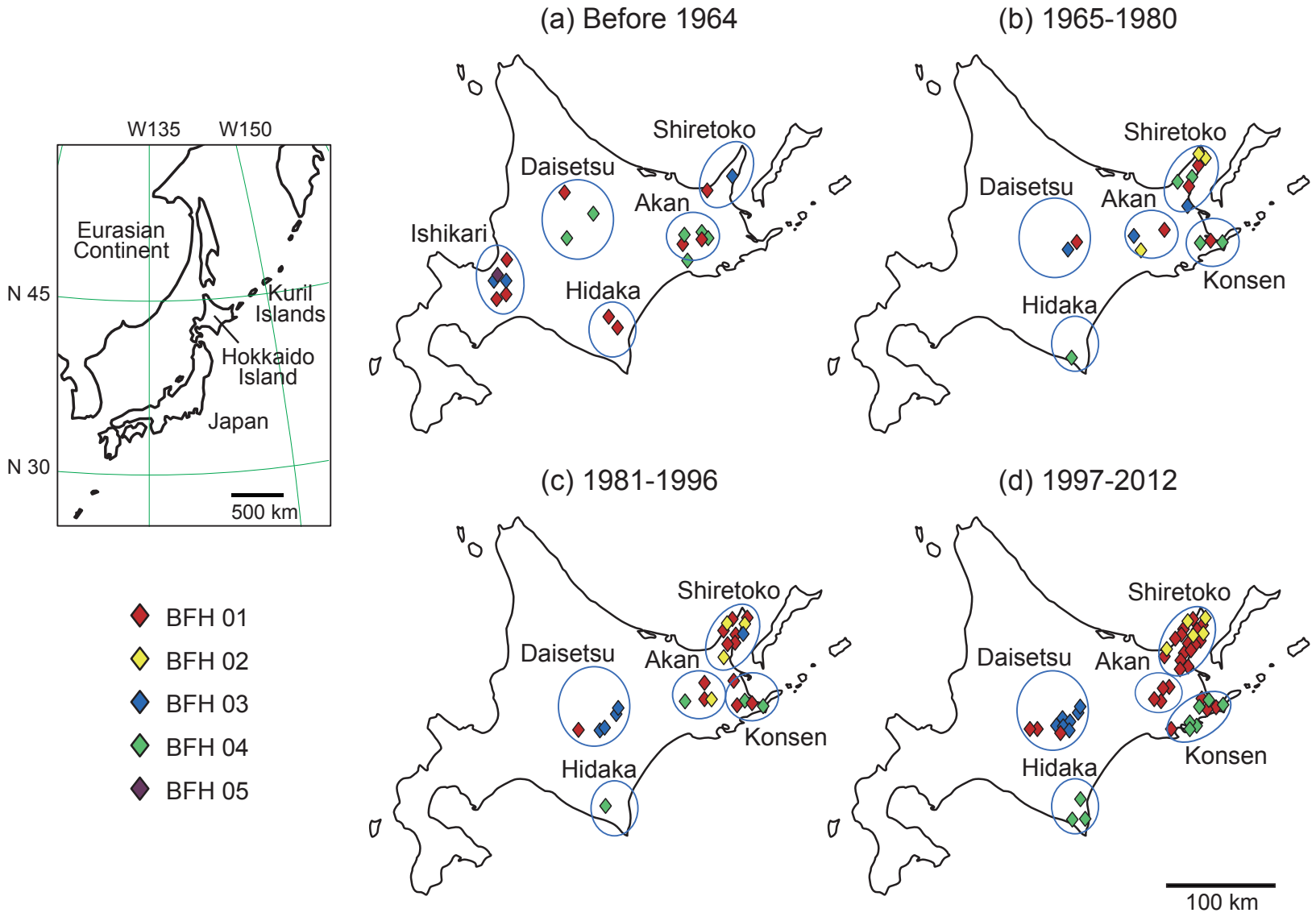

Fig. 3-1 Distribution of five mtDNA control-region haplotypes through time for Blakiston's fish owl on Hokkaido Island from Omote et al. (2015): (a) before 1964, (b) in intervals 1965–1980, (c) 1981–1996 and (d) 1997–2012. Color codes at the lower left indicate the haplotypes shared by individual owls. The map at the upper left shows the location of Hokkaido Island in eastern Asia.

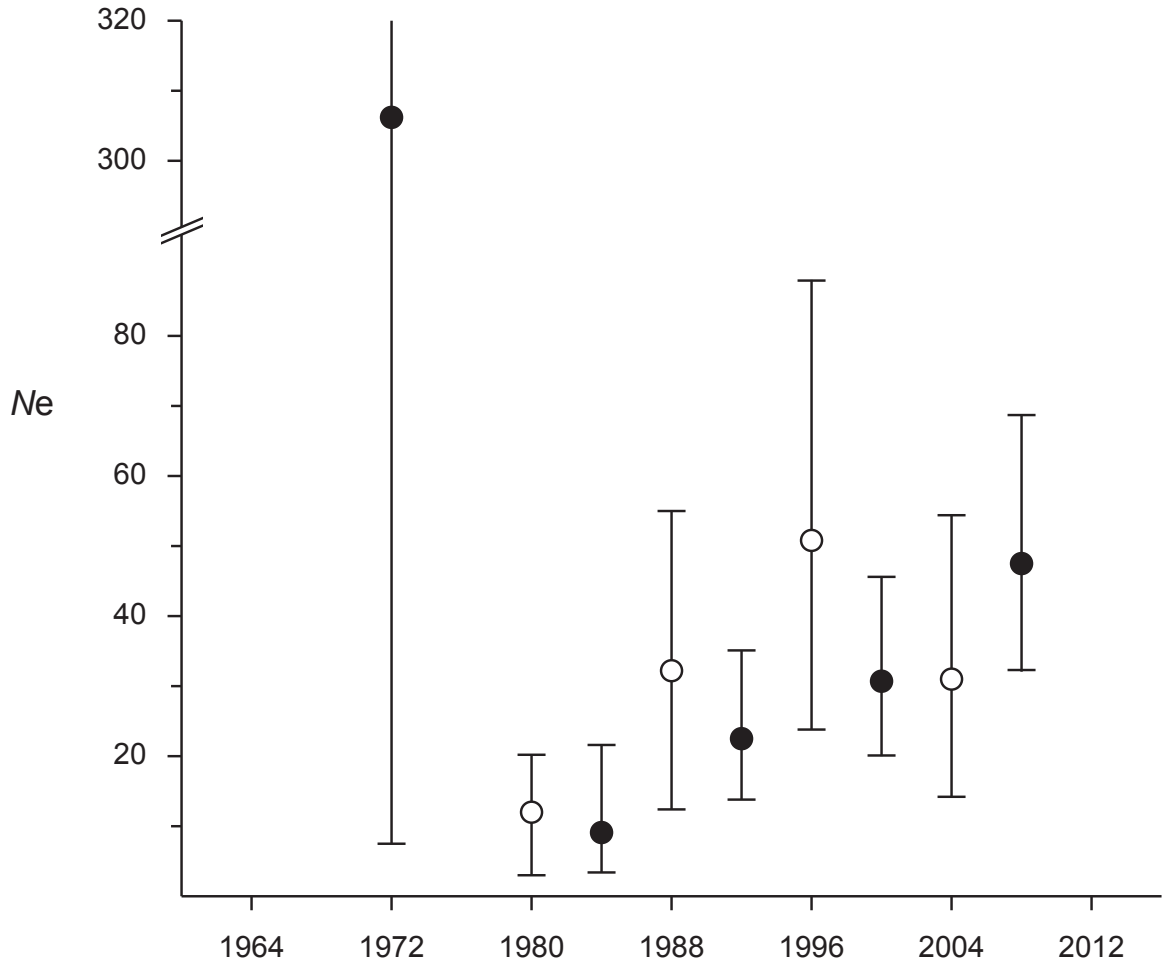

Fig. 3-2 Effective population sizes (*N*e) estimated by moment method (filled circles) for each period and temporal method (open circles) between continual periods from Omote et al. (2015). Error bars indicate 95% confidence intervals.

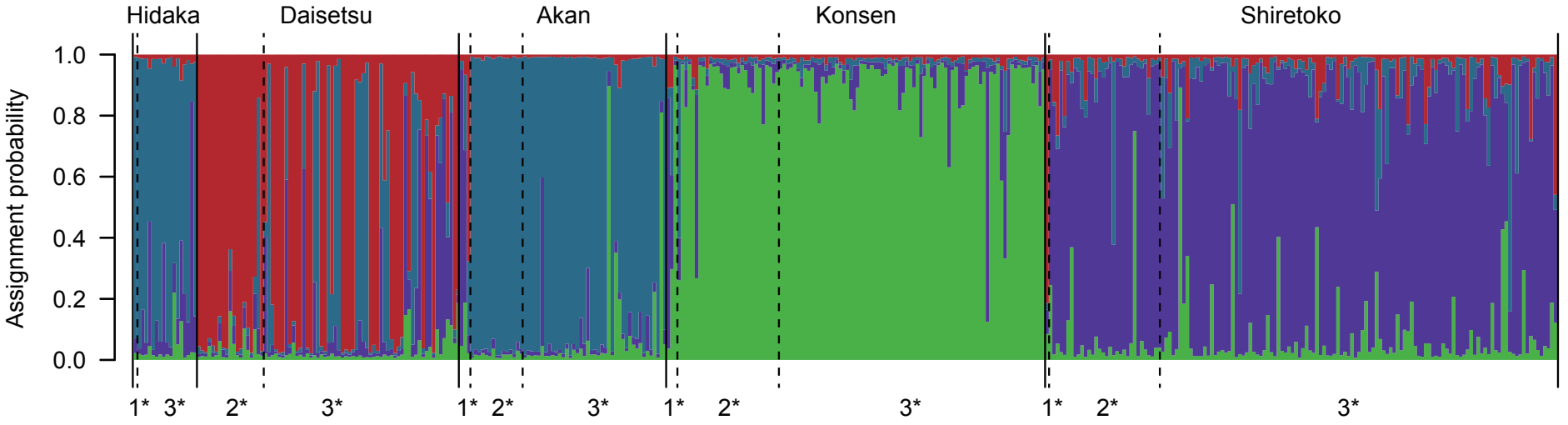

Fig. 3-3 Bar plots ($K = 4$) from the STRUCTURE analysis to determine the number of genetic clusters that best fit the microsatellite data for Blakiston's fish owl on Hokkaido from Omote et al. (2015). Each vertical line represents one individual, which is partitioned into four colored segments including the probability of assignment to each cluster. The individuals in each of the five local populations are arranged by sampling period: 1^*, 1965–1980; 2^*, 1981–1996; 3^*, 1997–2012.

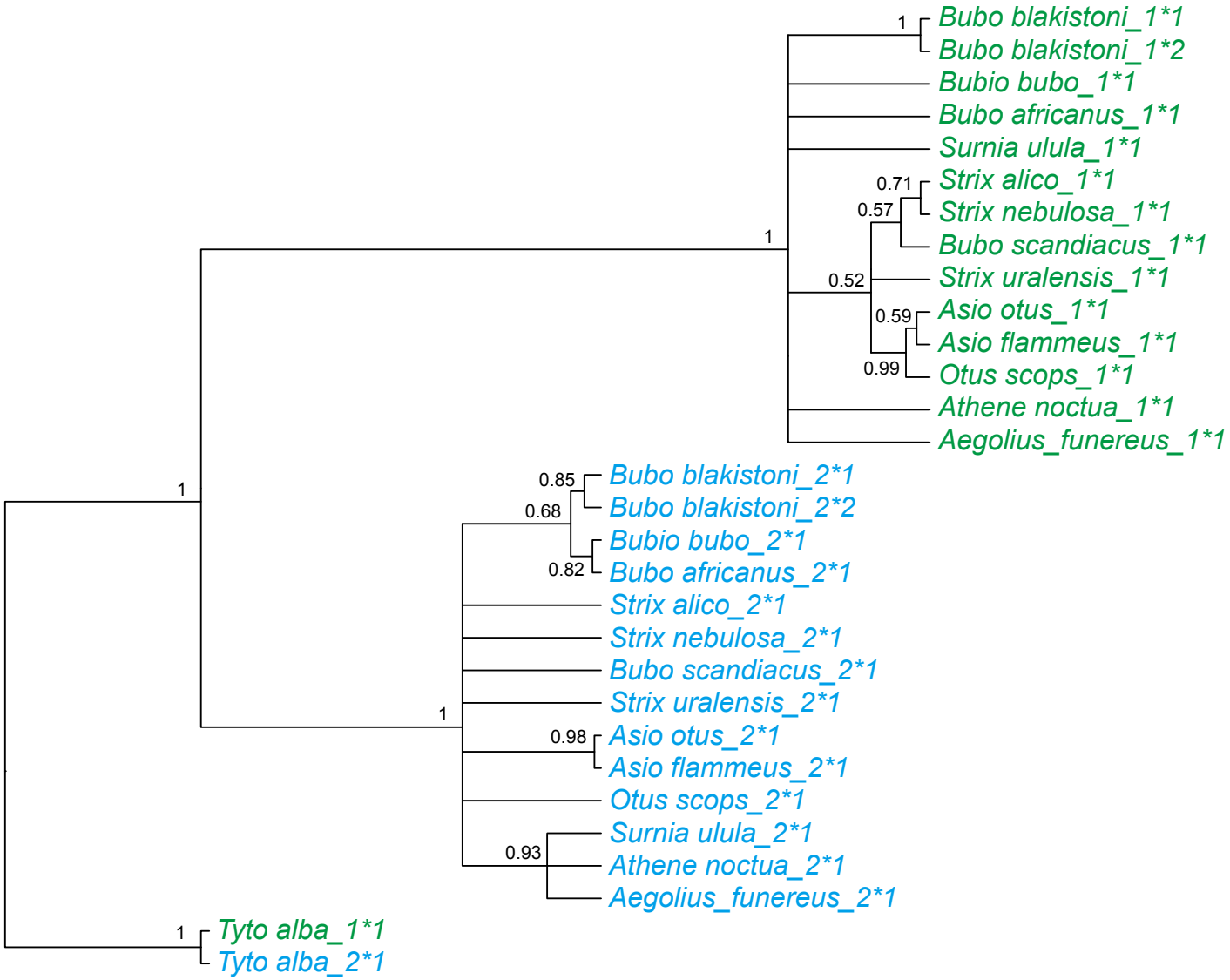

Fig. 4-1 Phylogenetic relationships among alleles of owl species based on MHC class IIβ exon 3 by the Bayesian analysis. Green and blue letters refer to DAB1 and DAB2 alleles, respectively. The posterior probabilities are shown on blanches. Species names correspond with those in "Materials and Methods" in the text.

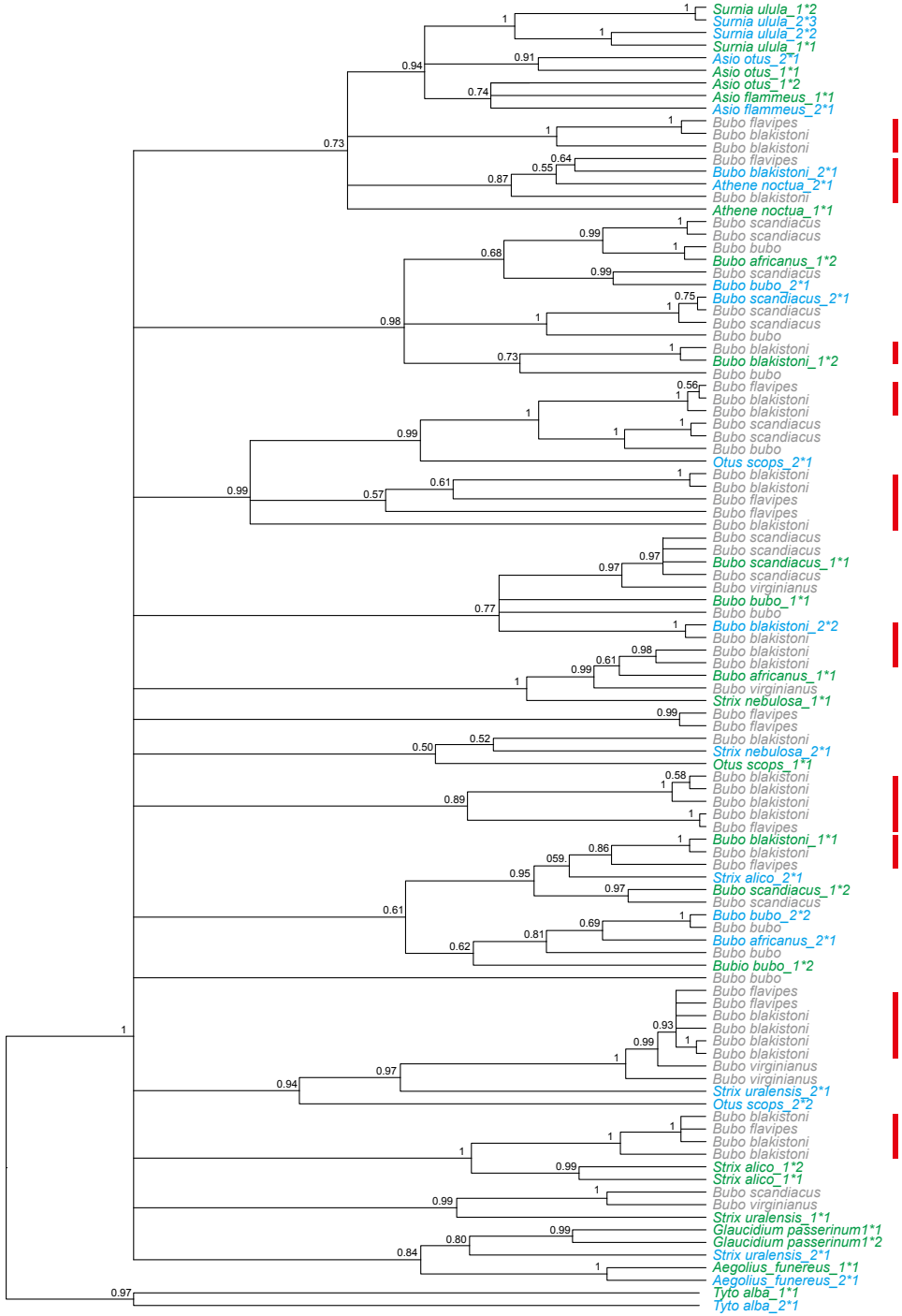

Fig. 4-2 Phylogenetic relationships among alleles of owl species based on MHC class IIβ exon 2 by the Bayesian analysis. Green and blue letters refer to DAB1 and DAB2 alleles, respectively, and grey letters refer to non-defined alleles because of lack of exon 3. The posterior probabilities are shown on blanches. The red bars show alleles of *B. blakistoni* and *B. flavipes*.

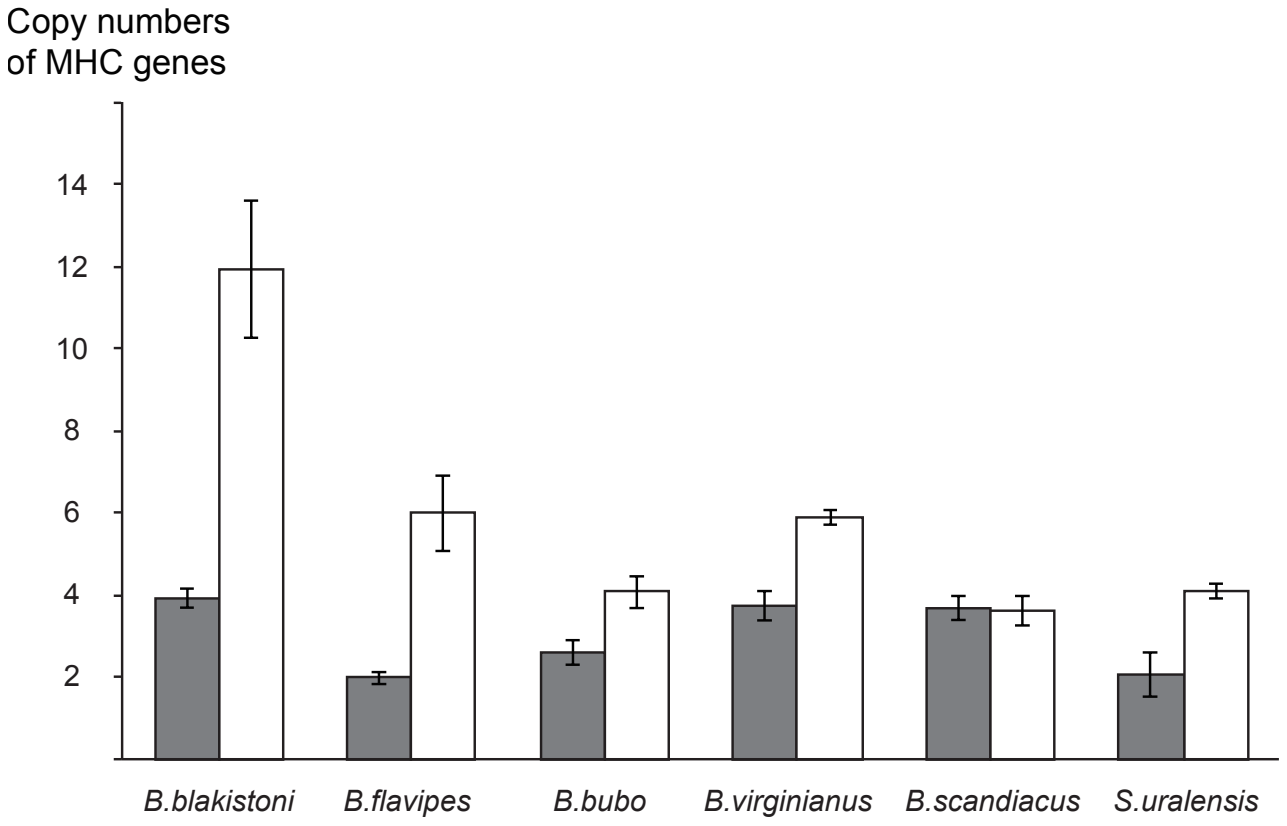

Fig. 4-3 Estimated numbers of gene loci by quantitative real-time PCR. Grey and white bars refer to MHC class I and class IIβ genes, respectively. The error bars show standard deviations.

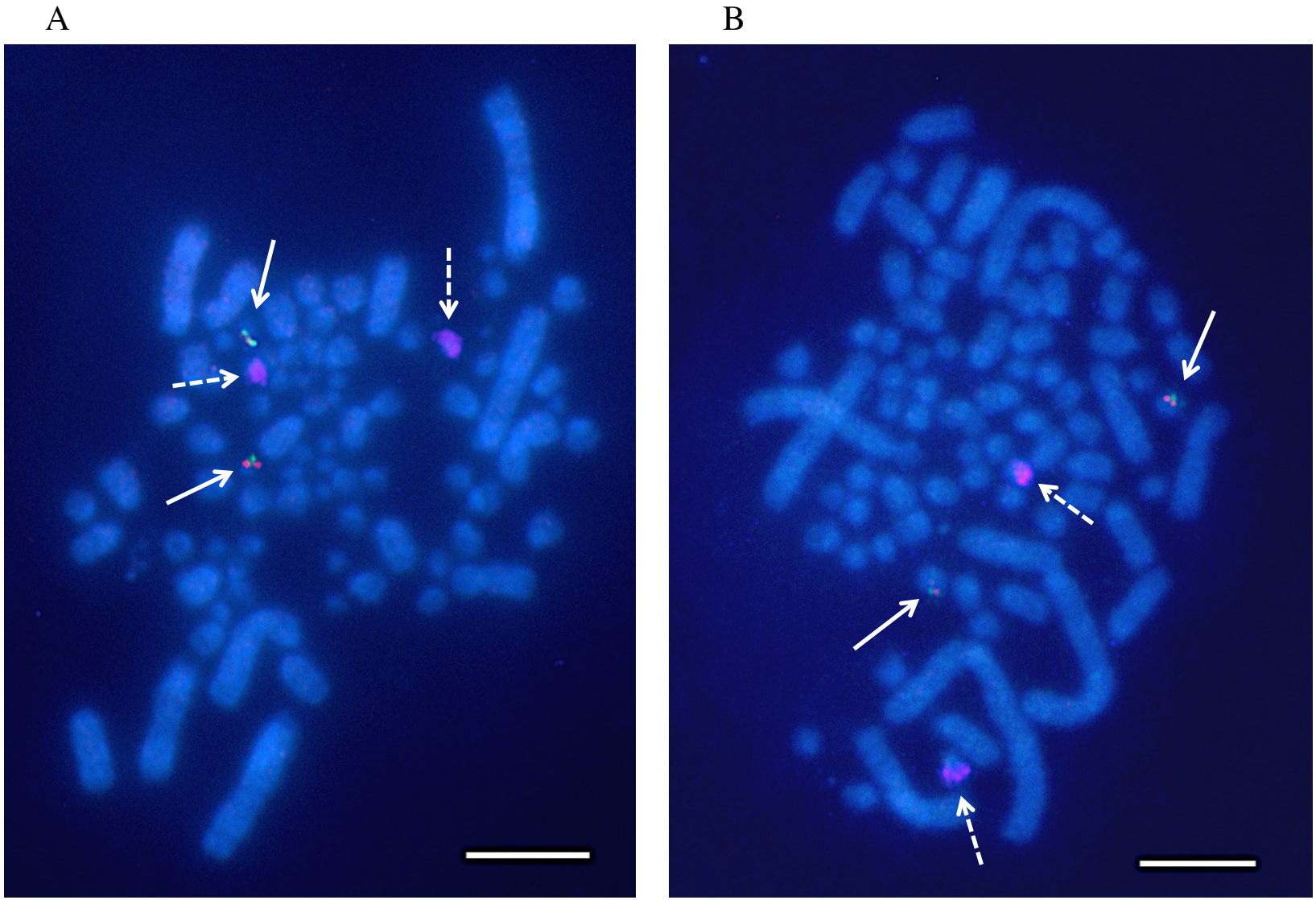

Fig. 4-4 FISH mapping of MHC class I (red), MHC class II (green) and 18S and 28S rRNA (purple) on chromosomes of *B. blakistoni* (A) and *B. bubo* (B). Allows with solid lines show MHC loci, and those with broken lines show 18S and 28S rRNA loci. Scale bars = 10 μm.

Table 1-1 Profiles of *Bubo* samples examined in the present study

Species		n	Tissue	Source
B. blakistoni	Blakiston's fish owl	20	Blood, Fibroblasts	wild-caught in Hokkaido
B. ketupa	buffy fish owl	1	Feather	Matsue Vogel Park
B. flavipes	tawny fish owl	1	Fibroblasts	Ueno Zoological Gardens
B. lacteus	Verreaux's eagle-owl	1	Feather	Matsue Vogel Park
B. nipalensis	spot-bellied eagle-owl	1	Feather	Ueno Zoological Gardens
B. sumatranus	barred eagle-owl	1	Feather	Ueno Zoological Gardens
B. bubo	Eurasian eagle-owl	2	Fibroblasts	Tama Zoological Park
B. virginianus	great horned owl	2	Fibroblasts	Sapporo Maruyama Zoo
B. scandiaca	snowy owl	2	Fibroblasts	Sapporo Maruyama Zoo
S. uralensis	ural owl	2	Fibroblasts	Kushiro City Zoo

Table 1-2 Primers for amplification and sequencing of owl mtDNA genes

Primers	Nucleotide sequence (5'-3') *	Locus	Citation
Lcontrol-01-kb	AGCCACGAATTGCTCGTTGTAC	Control region	This study
Lcontrol-02-kb	ATTCGTAAATTAAACCCAAACTC	Control region	This study
Hcontrol-03-kb	TGAAGAGTTATGGTTTAGGTACG	Control region	This study
Lcontrol-10-kb	CTTCTCACGTGAAATCAGCAACC	Control region	This study
Hcontrol-11-bl	AGATGGTCCTGACCGAGGAAC	Control region	This study
H01251	TCTTGGCATCTTCAGTGCCATGC	$tRNA^{Phe}$	Sorenson et al. (1999)
H01530	GTGGCTGGCACAAGATTTACC	12S rRNA	Sorenson et al. (1999)
H01858	TCGATTATAGGACAGGCTCCTCTAC	12S rRNA	Sorenson et al. (1999)
L14080	AACCCATGCCTTCTTCAAAGCC	ND5	Sorenson et al. (1999)
L14649	GGCTACTTCAACCCCCTAATACACC	ND5	Sorenson et al. (1999)
L15560	GTGACAAAATTCCATTCCACCC	Cytochrome *b*	Sorenson et al. (1999)
H16064	CTTCATTCTTTGGTTTACAAGACC	$tRNA^{Thr}$	Sorenson et al. (1999)
L16728	CCAAGGTCTGCGGCTTGAAAAG	$tRNA^{Glu}$	Sorenson et al. (1999)

* Underlines show the nucleotides revised from sequences reported by Srenson et al. (1999).

Table 2-1 Primers for PCR and sequencing

Primer	Nucleotide sequence (5'-3')	Position	Citation
H1251	TCTTGGCATCTTCAGTGCCATGC	tRNA-Phe	Sorenson et al. 1999
L1753	AAACTGGGATTAGATACCCCACTAT	12S-rRNA	Sorenson et al. 1999
H1858	TCGATTATAGGACAGGCTCCTCTAC	12S-rRNA	Sorenson et al. 1999
L2258	CGTAACAAGGTAAGTGTACCGGAAGG	12S-rRNA	Sorenson et al. 1999
L2724	ACCGAGCCGAGTGATAGCTG	16S-rRNA	Sorenson et al. 1999
L3652	CCAGGGATAACAGCGCAATC	16S-rRNA	Sorenson et al. 1999
H3827	GATAGAAACCGACCTGGATTGC	16S-rRNA	Sorenson et al. 1999
L4017	CGAAAAGGCCCCAACATCGTAGG	tRNA-Leu	Sorenson et al. 1999
H4500	CTTCGTAGGAGATAGTTTGTG	ND1	Sorenson et al. 1999
Hnd1-01	CAAGAGGAAATGGCAGAGG	ND1	This study
Hnd1-02	CGGCGTATTCTACGTTAAATC	ND1	This study
L5191	GCTATCGGGCCCATACCCC	tRNA-Met	Sorenson et al. 1999
L5758	GGCTGAATAGCTGCCATCCTC	ND2	Sorenson et al. 1999
L6615	CCTCTGTAAAAAGGACTACAGCC	tRNA-Tyr	Sorenson et al. 1999
H6958	AGTCAGAAGCTTATATTGTTC	CO1	Sorenson et al. 1999
L7338	CAACATCTCTTCTGATTCTTCGG	CO1	Sorenson et al. 1999
L7956	CGTCGATACTCCGACTACCC	CO1	Sorenson et al. 1999
L9034	CAGCACTAGCCTTTTAAGCTA	tRNA-Lys	Sorenson et al. 1999
H9233	AAGAAGCTTAGGTTCATGGTCAG	ATP8	Sorenson et al. 1999
H9742	TGCTGTGAGGTTTGCTGTTAG	ATP6	Sorenson et al. 1999
H10236	CTGGAGTGGAAGAATGCTCAG	CO3	Sorenson et al. 1999
L10647	TTTGAAGCAGCCGCCTGATACTG	CO3	Sorenson et al. 1999
H10884	GGGTCGAAACCGCATTCGTATGG	ND3	Sorenson et al. 1999
Lnd4l-01	TCCACACGAACCCACGGCTCCGA	ND4L	This study
H11660	AGGGGGGAGGAGATTTGGTC	ND4	Sorenson et al. 1999
L12134	CCCAAAGCCCACGTAGAAG	ND4	Sorenson et al. 1999
L12976	CAAGAGCTGCTAACTCCTGCATCTG	tRNA-Ser	Sorenson et al. 1999
Hnd5-01	GAGGCTGTAGGTTGCAGTG	ND5	This study
Hnd5-02	CGGATAAGTAGGAAGATTCC	ND5	This study
Hnd5-03	GATGAACAGTATGGAGTATAG	ND5	This study
L14080	AACCCATGCCTTCTTCAAAGCC	ND5	Sorenson et al. 1999
L14649	GGCTACTTCAACCCCCTAATACACCG	ND5	Sorenson et al. 1999
L15560	GTGACAAAATTCCATTCCACCC	CYTb	Sorenson et al. 1999
Lcytb-01	AGCTGACTCAACCCTAGCTT	CYTb	This study
Hcytb-02	ACAAATGAAGAAGAATGAGGC	CYTb	This study
H16064	CTTCATTCTTTGGTTTACAAGACC	tRNA-Thr	Sorenson et al. 1999
L16206	CTTCATTCTTTGGTTTACAAGACC	ND6	Sorenson et al. 1999
L16728	CTTTTCAGGCCGCAGACCTCGG	tRNA-Glu	Sorenson et al. 1999
Lcontrol-01	AGCCACGAATTGCTCGTTGTAC	CR	Chapter 1
Lcontrol-02	ATTCGTAAATTAAACCCAAACTC	CR	Chapter 2
Hcontrol-03	TGAAGAGTTATGGTTTAGGTACG	CR	Chapter 3
Lcontrol-17	AAATACTTACTATTAATGTACTGC	CR-1	This study
Hcontrol-18	GTACATGAATATGTGTGTCGTTT	CR-1	This study
Lcontrol-19	TTACCATCAATGTGCTACG	CR-2	This study
Hcontrol-20	GATGGGTATGTCGTTCTGTC	CR-2	This study

Table 3-1 Numbers of Blakiston's fish owls examined, by sampling locations and

	Sampling locations						
Period	Ishikari	Hidaka	Daisetsu	Akan	Konsen	Shiretoko	Total
pre–1964	[6]	1 [1]	[3]	[3] 3*		[2]	19
1965–1980		[1]	[2]	3	3	1 [6]	16
1981–1988		[1]	2	3 [1]	7 [1]	4 [3]	22
1989–1996		1	17	12	21 [1]	29	81
1997–2004			25	21	36	44	126
2005–2012		17	29	20	39	70	175
Total	6	22	78	66	108	159	439

Numerals without brackets show numbers of tissue samples, and those with brackets indicate numbers of feather roots from stuffed samples. Asterisks indicate archeological bone samples.

Table 3-2 PCR primers for amplification and/or sequencing the Blakiston's fish owl mtDNA control region

Primer	Nucleotide sequence (5'–3')	Citation
L16728	CCAAGGTCTGCGGCTTGAAAAG	Sorenson et al. 1999
Hcontrol-03-kb	TGAAGAGTTATGGTTTAGGTACG	Chapter 1
Hcontrol-05-kb	GGGCATTAATGTCATGAAATTAG	This study
Lcontrol-06-kb	TACTAATCCATGCACTAATCCC	This study
Hcontrol-07-kb	GCCATGGATTGGAGTATTAATAG	This study
Lcontrol-08-kb	CAGTTGTACATTAAACCATCTAC	This study
Hcontrol-09-kb	GGCATGGATGTTATATCTTGGTG	This study
Lcontrol-12-kb	GTACTAATCACATACAATTCATG	This study
Lcontrol-14-M13f	GTAAAACGACGGCCAGCCATTAATGTGCTACGTAT/	This study
Hcontrol-15-M13f	GTAAAACGACGGCCAGATGGGATTAGTGCATGGAT	This study
Lcontrol-16-M13f	GTAAAACGACGGCCAGCCTATTCATGACAGAACGA	This study

Underlines indicate the attached sequences of M13-forward for sequencing.

Table 3-3 Genetic differentiations and diversities caluculated by mtDNA haplotype and microsatellite data for the periods indicated

	mtDNA haplotype						Microsatellite					
Period	n	*F* st	*h* all	*h* local	π all	π local	n	*F* st (95% CI)	*A* r	*H* o	*H* e	*F* is
pre-1964	19	0.05	0.68	0.59	0.0074	0.0066						
1965–1980	16	-0.150	0.78	0.70	0.0085	0.0075	8	-0.07 (-0.18–0.07)	3.7	0.59	0.58	-0.02
1981–1988	16	0.31*	0.65	0.38	0.0067	0.0058	17	0.06* (-0.03–0.15)	3.5	0.53	0.56	0.05
1989–1996	28	0.55*	0.71	0.38	0.0070	0.0035	81	0.19* (0.11–0.25)	3.3	0.52	0.55	0.05
1997–2004	31	0.49*	0.65	0.39	0.0063	0.0036	126	0.16* (0.12–0.19)	3.2	0.47	0.54	0.13
2005–2012	40	0.60*	0.59	0.28	0.0065	0.0028	175	0.13* (0.08–0.16)	3.3	0.51	0.53	0.05

The following parameters are given: number of samples analyzed (n), genetic differentiation among local populations (*F* st), haplotype diversity on the overall and local populations (*h* all and *h* local), nucleotide diversity on the overall and local populations (π all and π local), mean of allelic richness (*A* r), observed (*H* o) and expected heterozigosity (*H* e), and inbreeding coefficient (*F* is). Asterisks indicate statistical significance of the *F* st values ($P < 0.05$).

Table 3-4 Pairwise *F* st values among local populations in the 1997–2012 interval based on mtDNA haplotype (above) and microsatellite (below) datasets

	Hidaka	Daisetsu	Akan	Konsen	Shiretoko
Hidaka		0.583*	1.000*	0.136	0.893*
Daisetsu	0.170*		0.472*	0.210*	0.559*
Akan	0.181*	0.176*		0.527*	0.103
Konsen	0.188*	0.168*	0.173*		0.637*
Shiretoko	0.133*	0.101*	0.119*	0.090*	

sterisks indicate statistical significance of the Fst values (*P* <0.0

Table 4-1 Numbers of alleles per individual found by massively parallel pyrosequencing. The data of *B. blakistoni* was sited from Kohyama et al. (2015).

Species	No. of samples	No. of allele/individual		
		min	mean	max
B. blakistoni	174	8	11.7	16
B. flavipes	1	-	12	-
B. bubo	2	5	6	7
B. virginianus	2	3	3.5	4
B. scandiacus	1	-	7	-